

Conductivity Anisotropy in Shale-Free Sandstone¹

W. David Kennedy² and David C. Herrick³

ABSTRACT

The existence of conductivity anisotropy has implications for formation evaluations using Archie's model for relating formation water saturation to formation resistivity. Bulk anisotropy of sedimentary rocks can arise from the interleaving of rock units having differing electrical properties. For special core analysis, whole core is often selectively plugged in attempting to obtain homogeneous samples in the supposition that measurements taken on homogeneous samples will yield values representing typical reservoir properties. It is an article of faith that heterogeneous rocks composited from components similar to the homogeneous samples will exhibit physical properties predictably intermediate between the properties of the homogeneous samples. This is a reasonable belief that is demonstrably true for certain scalar parameters of the formation, for example porosity. Unfortunately, the direction-dependent properties of the formation do not behave in this intuitive manner. For example, we examine a two-component layered model sandstone for which the values of Archie's porosity exponent m and saturation exponent n for the composite rock have values that are very different from those of the individual components. The exact values of m and n for composite rocks depend not only upon their values of the constituent components

but also upon the relative volume fractions of the components, and the orientation at which the conductivity measurements are made. Estimates of m and n in layered rocks based on simple averaging are incorrect. The theoretical results are supported by the general variability in the resistivities of samples having similar porosities in the experiment that determines m , manifest as the commonly observed "scatter" in the formation resistivity factor–porosity plots, and as anomalously low values of saturation exponents ($n \approx 1$) often observed in aeolian sandstones.

Neglecting the existence of these effects (as has been, and is still, done) must result in a false sense of the accuracy of formation evaluations, as well as an unwarranted lack of confidence in results from the laboratory when they are in conflict with naïve preconceptions of how formation properties should behave in the aggregate. A theoretical understanding of this issue must, at a minimum, improve estimates of uncertainty in formation evaluations. There is a definite (but as yet unrealized) promise that these effects can be accounted for and properly weighted in formation evaluations based upon triaxial induction logging instrument responses.

INTRODUCTION

The electrical properties of reservoir rocks have been historically important because for most occurrences of hydrocarbons, resistivity anomalies are as close to the direct

detection of hydrocarbons as any measurement made from the borehole provides. Archie (1942) showed how to relate the resistivity of a reservoir rock to the volume of fluids contained in the rock. Archie's relationship is empirical; its predictive power depends upon a knowledge of curve-fitting

Manuscript received by the Editor on March 27, 2003; revised manuscript received on December 10, 2003.

¹Originally presented at the SPWLA 44th Annual Logging Symposium, June 22-25, Galveston, Texas, paper T

²ExxonMobil International Ltd., London, U. K.

³BakerHughes, Houston, U.S.A.

©2004 Society of Petrophysicists and Well Log Analysts. All rights reserved.

parameters known as the porosity¹ and saturation exponents, m and n respectively. These are determined in a laboratory from core-derived samples of the reservoir, and the resulting values are taken as typical for the entire suite of rocks in the reservoir. In the absence of core-measured values for Archie parameters the nominal values are taken as equal to two, as a rule of thumb—slightly reduced for softer or younger rocks, slightly increased for harder or older rocks. There is a long-standing recognition of the problem of reservoir heterogeneity at the core scale. As a result, when special core analysis for Archie parameters is an objective, cores are typically plugged where they appear to be as visually homogeneous, and hence isotropic, as possible. On the other hand, in practice it is not easy to find sedimentary rocks, even at the core-plug scale, that are actually visually homogeneous and isotropic. This raises the question of whether the measured values actually provide the desired parameter values. If they do not, do the Archie parameters determined from heterogeneous plugs represent an intuitively reasonable average of the properties of their constituents, leading to reasonable predictions of average water saturations, or are there unsuspected pitfalls in using them for interpretation?

A related question is why Archie's formation resistivity factor F is so poorly determined by the data used to infer it. That is, why do plots of porosity-formation resistivity factor data, used to determine m , exhibit so much scatter? Similar plots of water saturation-resistivity index used for the determination of n are usually well determined by the data. Of course, the latter values are determined from a more controlled experiment, performed as it is on a single core plug. The conventional answer to the question of why there should be so much scatter in the corresponding porosity-formation resistivity factor plot—that the plugs used are after all taken from different places along the core, having differing porosities, with more-or-less differing depositional and diagenetic histories—no doubt has elements of truth, but is too vague to argue.

The discovery in the 1980s that saturation exponents could exhibit “anomalously” low values, close to or even less than one, was unexpected. At first, the results of laboratory measurements were not accepted as being correct. Eventually it was understood that the laboratory results were not in error, and low n values, especially in aeolian sandstones, became accepted (LaTorraca and Hall, 1991). In other circumstances the saturation exponent can be

anomalously large, say four or greater (Herrick and Kennedy, 1996).

In this article we demonstrate that m and n in a layered sandstone medium have surprising properties, not intuitively obvious, and very different from what would be expected on the basis of volume weighted averages of m and n using the constituent components of the medium.

THEORETICAL DEVELOPMENT

Consider a laminated sand reservoir comprising alternating sand layers that differ in their petrophysical properties (Figure 1a). For simplicity let us consider only two distinct sand types in the discussions to follow, but the general, multicomponent case will be developed in an appendix. For purposes of this study we consider each of the two sands to be internally, or locally, isotropic (Figure 1b). We also assume that the Archie (e.g., m and n) and other petrophysical parameters (e.g., porosity φ , water saturation S_w , etc.) of the individual layers are known, regardless that in actual practice the layers may be below the resolution limit for special core analysis. For specificity we assign an index “1” to the first component of the two-component model, and assign to it properties appropriate to a “fine-grained” component, and an index “2” to the second component, which is assigned properties appropriate to a “coarse-grained” component. The presumed consequence of grain-size variation is that, all other conditions being identical, the fine-grained rock, with its greater mineral surface area exposed to brine, will have its initial porosity diminished more rapidly, and therefore to a greater degree, by diagenesis (e.g., cementation, compaction, etc.) than the otherwise similar coarse-grained rock. In other words, the fine-grained component is assumed to have a lower porosity than the coarse-grained component in this model.

The bulk horizontal conductivity σ_h of this medium as computed from the volume-weighted average of the conductivities of the two sand fractions, σ_1 and σ_2 , where both of the sands are locally homogeneous and isotropic, is

$$\sigma_h = \beta\sigma_1 + (1 - \beta)\sigma_2 \quad (1)$$

where β ($0.0 \leq \beta \leq 1.0$)² is the volume fraction of the fine-grained sand component. The bulk vertical conductivity σ_v is computed as the volume-weighted average of the reciprocal conductivities, viz.,

¹The porosity exponent has been known as the “cementation” exponent, but this is a misnomer that evokes misleading and confusing images in the mind’s eye. Use of “porosity” exponent for m is in parallel with the well-accepted use of “saturation” exponent for n . It does not suggest any physical process but merely names the term to which the exponent applies.

²A table of nomenclature is found following the Conclusions.

$$\frac{1}{\sigma_v} = \frac{\beta}{\sigma_1} + \frac{(1-\beta)}{\sigma_2}. \quad (2)$$

We wish to examine certain petrophysical properties, specifically Archie's parameters m , n , the formation resistivity factor F , and the resistivity index I , of a composite rock comprising layers below the limit of logging instrument resolution that therefore exhibits average (or bulk) properties that differ from the properties of the individual constituents.

You may note that the volume-weighted average (or bulk) porosity $\bar{\varphi}$ of the sand-package assembled from the two component sands is

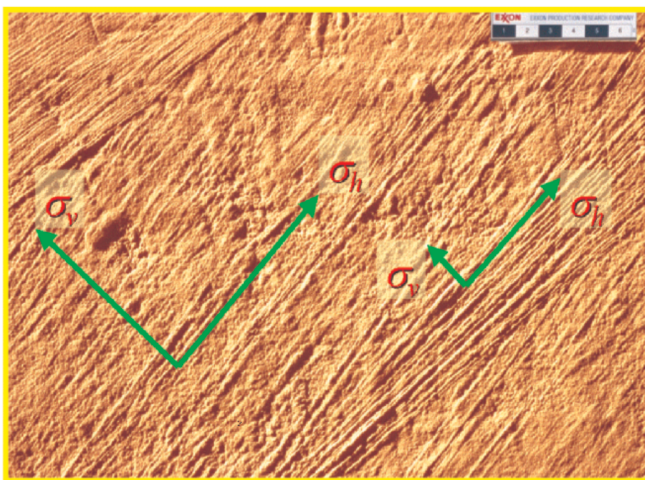


FIG. 1a A sand peel of a shale-free slip face of a modern dune trenched to show its structure. The scale divisions are in centimeters. The visible structure results from the differential uptake of the acrylic binding resin used to create the peel. The orientation is as observed in the field. As part of a reservoir, this sand unit would have a relative deviation of about 45 degrees with respect to a vertical borehole, regardless that the structural dip is zero. Conventional resistivity logs would be misinterpreted and hydrocarbon pore volume misquantified using conventional water saturation estimation techniques if this relative deviation is not accounted for. The visible lamina correspond to grain size differences. The coarsest grains correspond to highest energy of transport, the finest grains to the lowest energy. Between these end members are several intermediate grain sizes. The Archie parameters of this rock are not simple averages of the Archie parameters of the individual layers. The complication arises from the differential change in the conductivity as brine is replaced by hydrocarbons. This is illustrated by the coordinate frame on the left, the length of the axes corresponding to the conductivities parallel and perpendicular to laminations in a brine-saturated rock. The coordinate frame on the right illustrates that the replacement of brine with hydrocarbon reduces the perpendicular component of conductivity significantly more than the parallel component of conductivity.

$$\bar{\varphi} = \beta\varphi_1 + (1-\beta)\varphi_2 \quad (3)$$

and that the volume-weighted average brine content (Figure 1b) for the package will be

$$\overline{\varphi S_w} = \beta\varphi_1 S_{w1} + (1-\beta)\varphi_2 S_{w2}. \quad (4)$$

Now define $\overline{S_w}$ by $\overline{S_w} \cdot \bar{\varphi} \equiv \overline{\varphi S_w}$. From this definition and equation (4), the average (or bulk) water saturation will be

$$\begin{aligned} \overline{S_w} &= \frac{\beta\varphi_1 S_{w1} + (1-\beta)\varphi_2 S_{w2}}{\bar{\varphi}}, \\ &= \frac{\beta\varphi_1}{\beta\varphi_1 + (1-\beta)\varphi_2} S_{w1} + \frac{(1-\beta)\varphi_2}{\beta\varphi_1 + (1-\beta)\varphi_2} S_{w2}. \end{aligned} \quad (5)$$

$\overline{S_w}$ is also a volume-weighted average; the first term on the right side of (5) is the fraction of the porosity that belongs to the first porosity component multiplied by the water saturation in that component, while the second term on the right side of (5) is the fraction of the porosity that belongs to the second porosity component multiplied by the water satura-

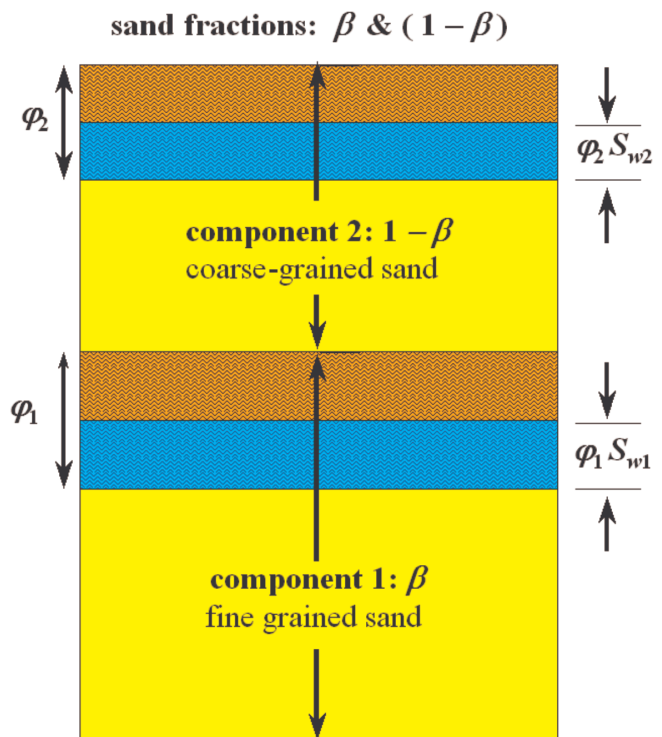


FIG. 1b A cartoon illustrating the components of a laminated sand package. The porosity and fluid fraction of each component has been lumped for purposes of easy illustration. The hydrocarbon fraction is color-coded brown.

tion in that component. Thus, in a sense (5) is a volume-weighted average of the brine content of the separate components. We will show that while σ_h , $1/\sigma_v$, $\bar{\varphi}$, and S_w and a few other petrophysical properties of the composite medium behave in this “intuitively obvious” manner for averages, the important properties of averaged m and n are more complicated.

DIRECTION-DEPENDENT FORMATION FACTORS: F_{\parallel} AND F_{\perp}

In a model rock composed from two components having porosities φ_1 and φ_2 present in the volume fractions β and $1 - \beta$, the parameter β is required explicitly in terms of the average porosity given in equation (3). This is¹

$$\beta = \frac{\varphi_2 - \bar{\varphi}}{\varphi_2 - \varphi_1}, \quad \text{where} \quad \varphi_1 \leq \bar{\varphi} \leq \varphi_2 \quad (6)$$

and where we have assumed for specificity that the fine-grained component has a lower porosity than the coarse-grained component. Archie’s “law,” usually expressed in terms of resistivity as $R_t = R_w FI = R_w \cdot 1/\varphi^m \cdot 1/S_w^n$ where all of the symbols have their conventional meanings, is expressed in terms of conductivity as $\sigma_t = \sigma_w \varphi^m S_w^n$ where the subscripts and exponents retain their conventional meanings and conductivity $\sigma = 1/R$ is reciprocal resistivity. When hydrocarbons are not present in the formation, by convention the subscript t is changed to 0. The parameters corresponding to one or the other component are distinguished by the use of subscripts, 1 and 2.

Consider the case where $S_w = 1.0$. In equation (1) substituting $\sigma_1 = \sigma_w \varphi_1^{m_1}$ and $\sigma_2 = \sigma_w \varphi_2^{m_2}$, and dividing by the connate water conductivity σ_w , results in

$$\frac{\sigma_h}{\sigma_w} = \frac{\sigma_{\parallel}}{\sigma_w} = \beta \varphi_1^{m_1} + (1 - \beta) \varphi_2^{m_2} = \frac{R_w}{R_{\parallel}} = \frac{1}{F_{\parallel}} \quad (7)$$

where the subscript \parallel (read “parallel”) indicates properties sampled parallel to laminations. In flat-lying beds this component may happen to be “horizontal” and often is given a subscript h , but not all laminations are oriented in this simple way. The “ \parallel ” notation avoids possible ambiguity in the interpretation of “horizontal.” Thus

$$F_{\parallel} = \frac{1}{\beta \varphi_1^{m_1} + (1 - \beta) \varphi_2^{m_2}} \equiv \frac{1}{\bar{\varphi}^{m_1}} \quad (8)$$

where the definition of m_{\parallel} at the right end of (8) is made by

analogy with the corresponding Archie relationship. F_{\parallel} and $\bar{\varphi}$ are obtained from laboratory resistivity measurements made in the usual way.

Making the same substitutions as made in equation (2) will lead to

$$\frac{1}{\sigma_v} = \frac{1}{\sigma_{\perp}} = \frac{\beta}{\sigma_w \varphi_1^{m_1}} + \frac{1 - \beta}{\sigma_w \varphi_2^{m_2}} \quad (9)$$

or

$$\frac{\sigma_w}{\sigma_{\perp}} = \frac{\beta}{\varphi_1^{m_1}} + \frac{1 - \beta}{\varphi_2^{m_2}} \equiv F_{\perp} \quad (10)$$

$$F_{\perp} = \frac{\beta \varphi_2^{m_2} + (1 - \beta) \varphi_1^{m_1}}{\varphi_1^{m_1} \varphi_2^{m_2}} \equiv \frac{1}{\bar{\varphi}^{m_1}} \quad (11)$$

where the subscript \perp (for perpendicular) indicates properties sampled perpendicular to bedding planes or laminations, avoiding ambiguity in the use of the word “vertical.” Again, the definition at the right end is suggested by the analogous Archie relationship. In equations (6)–(11), notice that $\bar{\varphi}$ is a scalar property while F_{\parallel} , m_{\parallel} , F_{\perp} , and m_{\perp} are all direction-dependent. (These defining relations are listed in Appendix A)

ARCHIE’S POROSITY EXPONENT m

In terms of average properties the Archie relations for the bulk medium are direction-dependent. In the equations expressing the relations, if one side is direction-dependent, then of course, both sides must be direction-dependent. That is, considering equations (8) and (11), if F_{\parallel} and F_{\perp} are direction-dependent but φ (and $\bar{\varphi}$) and S_w (and S_w) are not direction-dependent, then the saturation exponent n and porosity exponent m , as the only parameters remaining on the right side of the equations, necessarily have to be the direction-dependent factors in Archie’s relations connecting resistivity to porosity and water saturation. For example, for the horizontal direction, in terms of conductivity, from equation (1) we have the composite conductivity parallel to the bedding planes

$$\begin{aligned} \sigma_{t_{\parallel}} &= \beta \sigma_1 + (1 - \beta) \sigma_2 = \sigma_w \bar{\varphi}^{m_1} \bar{S}_w^{n_1} \\ &= \sigma_w (\beta \varphi_1^{m_1} S_{w_1}^{n_1} + (1 - \beta) \varphi_2^{m_2} S_{w_2}^{n_2}). \end{aligned} \quad (12)$$

Equation (12) provides the definition of the porosity and saturation exponents parallel to the bedding planes. In the

¹If φ_1 and φ_2 are distributed in layers thinner than can be resolved by a logging instrument, $\bar{\varphi}$ corresponds to a “porosity” logging instrument response.

case of $S_{w_1} = S_{w_2} = 1.0$ the relation between the bulk horizontal conductivity and the sand fractions would be

$$\sigma_{0\parallel} = \beta\sigma_w\varphi_1^{m_1} + (1-\beta)\sigma_w\varphi_2^{m_2} = \sigma_w\bar{\varphi}^{m\parallel}. \quad (13)$$

Thus

$$\bar{\varphi}^{m\parallel} = \beta\varphi_1^{m_1} + (1-\beta)\varphi_2^{m_2} = \frac{\sigma_{0\parallel}}{\sigma_w}, \quad (14)$$

leading finally to a solution for $m\parallel$,

$$m\parallel = \frac{\ln(\beta\varphi_1^{m_1} + (1-\beta)\varphi_2^{m_2})}{\ln\bar{\varphi}}. \quad (15)$$

$m\parallel$ applies to conductivity measurements that are made parallel to the bedding planes. Similarly

$$\frac{1}{\sigma_\perp} = \frac{1}{\sigma_w\bar{\varphi}^{m\perp}\bar{S}_w^{n\perp}} = \frac{\beta}{\sigma_w\varphi_1^{m_1}S_{w_1}^{n_1}} + \frac{1-\beta}{\sigma_w\varphi_2^{m_2}S_{w_2}^{n_2}}. \quad (16)$$

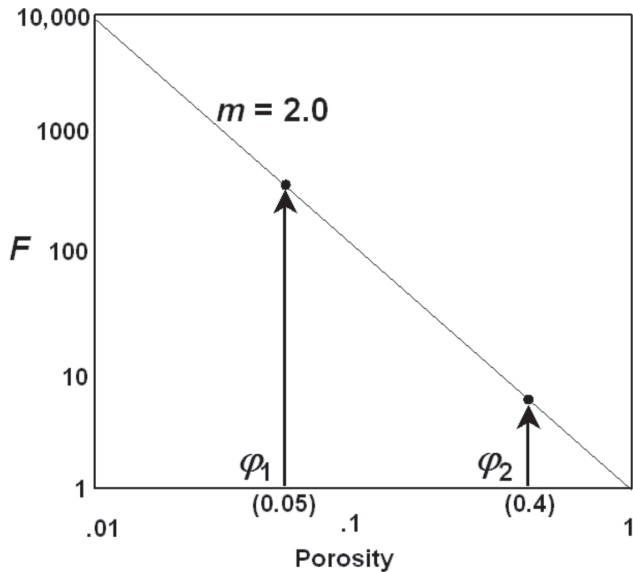


FIG. 2 A simple two-component composite rock model. Consider a sand package comprising layers of two distinct types of sand. Both sands have formation resistivity factors that fall along the $m = 2$ line of a formation-resistivity factor–porosity plot. In other words, although the porosity varies, the Archie parameters are the same for each type of rock. Obviously, the porosity of the composite rock is the volume-weighted average of the two components. But, what is the porosity exponent m for the composite?

Proceeding with a solution for this equation for $m\perp$,

$$\frac{1}{\bar{\varphi}^{m\perp}\bar{S}_w^{n\perp}} = \frac{\beta\varphi_2^{m_2}S_{w_2}^{n_2} + (1-\beta)\varphi_1^{m_1}S_{w_1}^{n_1}}{\varphi_1^{m_1}S_{w_1}^{n_1}\varphi_2^{m_2}S_{w_2}^{n_2}} \quad (17)$$

then

$$\bar{\varphi}^{m\perp}\bar{S}_w^{n\perp} = \frac{\varphi_1^{m_1}S_{w_1}^{n_1}\varphi_2^{m_2}S_{w_2}^{n_2}}{\beta\varphi_2^{m_2}S_{w_2}^{n_2} + (1-\beta)\varphi_1^{m_1}S_{w_1}^{n_1}}. \quad (18)$$

For the case $S_{w_1} = S_{w_2} = 1.0$

$$\bar{\varphi}^{m\perp} = \frac{\varphi_1^{m_1}\varphi_2^{m_2}}{\beta\varphi_2^{m_2} + (1-\beta)\varphi_1^{m_1}}, \quad (19)$$

and finally

$$m\perp = \frac{\ln\left(\frac{\varphi_1^{m_1}\varphi_2^{m_2}}{\beta\varphi_2^{m_2} + (1-\beta)\varphi_1^{m_1}}\right)}{\ln\bar{\varphi}^{m\perp}} \quad (20)$$

where $m\perp$ applies to conductivity measurements that are made perpendicular to the bedding planes.

VARIATION OF m IN A TWO-COMPONENT SANDSTONE

Figures 2 and 3 illustrate a hypothetical and near-canonical¹ experiment of determining the porosity exponent parameter in a resistivity experiment. The resistivity of two brine-saturated isotropic rocks, having different porosity but sharing identical Archie parameters, is plotted as shown on a log-log plot. These rocks represent the end members of an ensemble of layered composite rocks made of all possible volume fractions of the end members. Composite rocks in this ensemble have porosities between 5 and 40 percent. These values are chosen to represent the entire porosity range between a point near the percolation threshold and a point near the disaggregation limit. At the percolation threshold the conducting brine becomes a discontinuous phase. At the disaggregation limit the rock-forming mineral becomes a discontinuous phase. Since these represent the hypothetical limiting cases, results using them should encompass all measurements taken on “real” rocks. This obviously means that when observed in actual data, the effects will typically be smaller than those presented for limiting cases.

¹A particular choice from a number of possible conventions. This convention allows a mathematical object or class of objects to be uniquely identified or standardized. For example, the right-hand rule for the cross product is a convention, which corresponds to the *canonical* orientation in \mathbb{R}^3 (Euclidian three-space).

In the Archie experiment, values of formation resistivity factor ($= R_0/R_w$) are plotted against φ on a log-log grid and a line is fitted through the resulting cloud of points. In this example only two points are considered. The canonical value of the slope of the line is 2. Figure 3 illustrates a more realistic situation where the slope departs from the canonical value of 2. In younger, softer, higher porosity rocks, the value of the porosity exponent tends to be less than 2. In older, harder, lower porosity rocks, the value of the porosity exponent tends to be greater than 2. Figure 3 shows the cases of a line determined on two samples, one having a porosity exponent of 1.8 and the other having a porosity exponent of 2.3. We now propose a *gedanken* (i.e., thought) experiment. Construct a laminated rock comprising two

components: one component has 5 percent porosity and lies on the trend for $m = 2.3$ while the other component has 40 percent porosity and lies on the trend for $m = 1.8$. For Figures 2 and 3 imagine the relative proportions of the two constituents to vary over the entire range of possible volume fractions. What will be the resulting porosity exponent for such a composite rock? The slope of the lines connecting the two end members in Figures 2 and 3 offers a possible answer to this question. Is it a correct answer?

To resolve the issue analytically, begin with the consideration of the simpler case of the composite rock with end members that are both limiting elements of what we shall call the “canonical ensemble¹.” That is, consider two sandstone components having differing porosities of 5 and 40 percent but having the same porosity exponent, $m = 2$. If we composite the gedanken rock from *these* components, many properties of the composite will be volume-weighted averages of the end members. Assuming this to be true of the porosity exponent, then it seems intuitively obvious that the porosity exponent of the composite rock will lie on the canonical $m = 2$ line for the points in Figure 2, or a line connecting the $m = 2.3$ point to the $m = 1.8$ point for the two points in Figure 3. This may be an obvious assumption to adopt, but it is not correct.

Figure 4 shows the results of using equations (8) and (11) to compute the formation resistivity factors parallel and perpendicular to the bedding planes. The dashed magenta line marks $m = 2$ on the plot. The coordinates of the end member components are circled in red. As fractional volume is varied between the end members, the formation resistivity factor measured parallel to the bedding planes follows the path traced by the lower red curve. Measured perpendicular to the bedding planes, the formation resistivity factor follows the path traced by the upper blue curve. An envelope (the two green lines) is drawn from the “brine point” (i.e., $\varphi = 1.0, F = 1.0$) through the upper and lower tangents to the functions. The result shows that depending on the orientation of the sample and the volume fraction of the components, the composite rock can have porosity exponents that vary from $1.6 < m < 4.0$. Figure 5 plots the same data in a more dramatic diagram that shows the porosity exponent

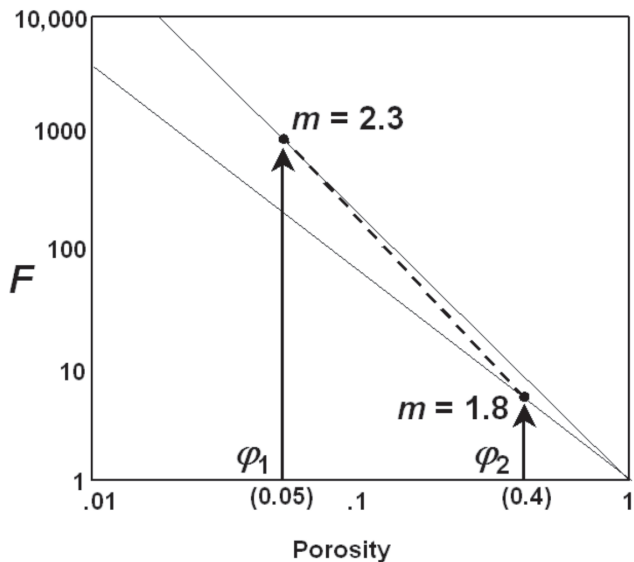


FIG. 3 A more realistic two-component composite rock model. In this case, the Archie m parameter varies with the porosity as it might be expected to do in some real rocks. The low-porosity fraction is assigned $m = 2.3$; the higher porosity fraction is assigned $m = 1.8$. In an anisotropic rock composed from these two fractions, you might expect the slope of the formation resistivity factor porosity line to vary linearly between the end points. However, the actual variation is more interesting.

¹The term ensemble is borrowed from the statistical mechanical lexicon where it is asserted that consideration of the state of a random process as a function of (a very long) time is equivalent to looking at a (very large) number of identical random processes (started with differing initial conditions) at the *same* time. The “large number” is referred to as an ensemble. The assertion holds for what are called stationary, or “ergodic,” processes. In petrophysics, rather than watch the history of porosity changes in a single core sample from the time of deposition to the time of coring, we simultaneously (in the “geological time” sense) consider an ensemble of samples that happen to be different points in their histories as representative of the process of porosity change with diagenesis. As used here, a canonical ensemble is the set of all possible laminated-sand models composed from a locally isotropic, fine-grained sand component with fractional volume β having porosity = 0.05 and having $m = n = 2$, and a locally isotropic, coarse-grained sand component with fractional volume $1 - \beta$ with a porosity = 0.40 and having $m = n = 2$. For the component porosity and saturation exponents chosen (equal to 2 for both parameters in both components), the entire possible range of variation in m and n due to porosity, water saturation, and *volume fraction* variation in laminated sandstones is contained within this set.

plotted against the volume fraction of the rock components. From this you can see that the average porosity exponent of the composite rock does not conform to any naïve notion of the expected behavior of this rock property.

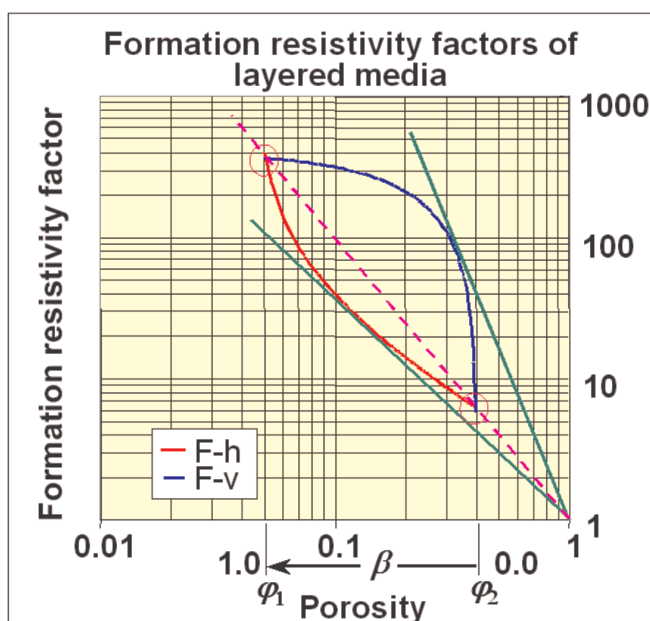
Figures 6 and 7 are similar to Figures 4 and 5, except that the end members of the composite are selected from rocks having the different, more realistically chosen, porosity exponents illustrated in the Figure 3 model. In this case the porosity exponent satisfies $1.5 < m < 4.75$.

Because in practice the measurement of m is always attempted parallel to the bedding planes, the range of variability will typically be less than the maximum ranges indi-

cated above. It is natural to question whether rocks composed of end members, each having $m = 2$, could be said to have a variation in porosity exponent limited to the range $1.6 < m < 2.0$. This is true to the degree that measurements are successfully aligned with the bedding planes. But, considering the model illustrated in Figures 2, 4, and 5, for a misalignment of 30° , depending upon the relative volume fractions of the components, it can be shown that $m \approx 2.2$ (for $\beta \approx 0.1$) or $m \approx 1.7$ (for $\beta \approx 0.9$). Intuition, founded as it is in linear variations, is not a useful guide. These estimates are supported by computations based on the analysis given in Appendix B.

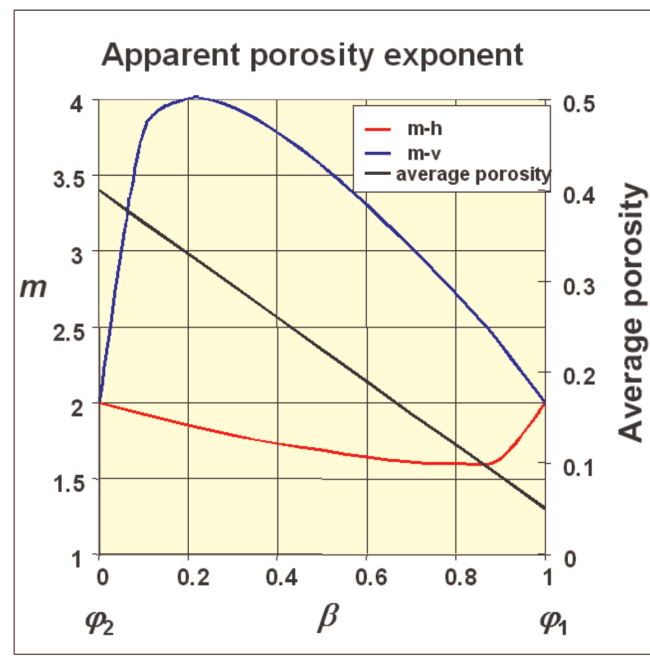
Of course, when the end members of the composite are more similar in porosity than $\varphi_1 = 0.05$ and $\varphi_2 = 0.40$, the effects of fractional composition and measurement alignment are diminished. But, that is not to say that there are no practical consequences.

The gedanken experiment strongly suggests that the customary procedure of selectively acquiring the core plugs used in special core analysis in the most homogeneous units



$$\begin{aligned} \varphi_1 &= 0.05, & m_1 &= 2.0 \\ \varphi_2 &= 0.40, & m_2 &= 2.0 \end{aligned}$$

FIG. 4 A hypothetical reservoir exhibiting a formation-resistivity factor–porosity function with a slope of $m = 2$. The locus of points with $m = 2$ is indicated by the dashed magenta line. The porosity end members have $\varphi = 0.05$ (presumed fine-grained) and $\varphi = 0.40$ (presumed coarse-grained), respectively. These end members are circled in red. The direction of increasing β and the end points of the β scale are shown for reference. For a laminated sand built from the end members in various proportions, how does m vary? The lower (red) line shows the locus of points for the parallel component of the formation resistivity factor as the fractional volume of the components varies from 0 to 100 percent. The upper line (blue) is the locus of points for the perpendicular component of the formation resistivity factor as the fractional volume of the components varies from 0 to 100 percent. The green lines bound the envelope of m values. From the slopes of the green lines we find that $1.6 \leq m \leq 4.0$ approximately.



$$\begin{aligned} \varphi_1 &= 0.05, & m_1 &= 2.0 \\ \varphi_2 &= 0.40, & m_2 &= 2.0 \end{aligned}$$

FIG. 5 A comparison of the porosity exponent m measured in the horizontal and vertical directions. Although the sand package is composed from individual sands with $m = 2$, the composite has m values quite different from 2. The red curve is for the component of m measured parallel to bedding planes, and the blue curve is the component of m measured perpendicular to bedding planes.

visible in the whole core, if it is entirely successful, will *not* lead to correct predictions of the porosity exponents that are representative of nearby laminated rocks composed from the homogeneous components if simple, volume-weighted arithmetic averaging is used in the prediction. On the other hand, given the difficulty in identifying such homogeneous units, a possible cause (in addition to many other causes that have been postulated) for the often-observed “scatter” in these data is a failure to control the experiment for the variability of laminations among the plugs in a set of samples.

DIRECTION-DEPENDENT RESISTIVITY INDICES: I_{\parallel} AND I_{\perp}

We now consider the conductivity behavior of the composite rock for cases where $S_w < 1.0$. The resistivity index is defined as

$$I = \frac{R_t}{R_0} = \frac{\sigma_0}{\sigma_t} = S_w^{-n}. \quad (21)$$

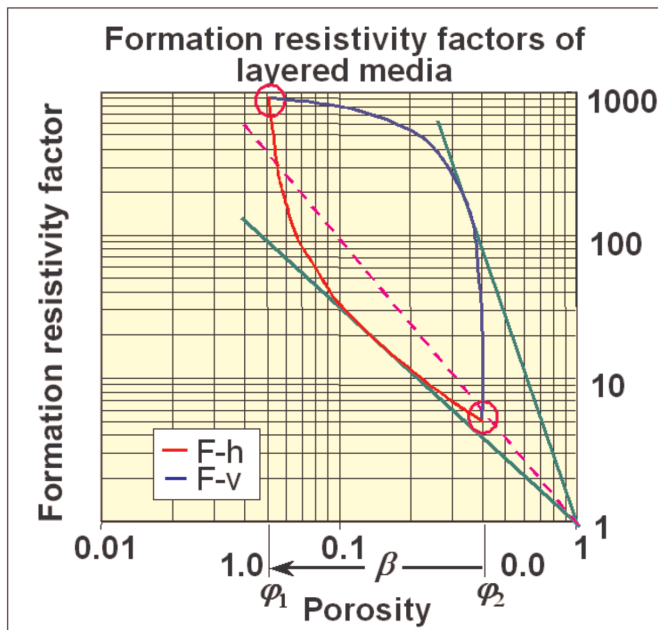


FIG. 6 Variation of the Archie porosity exponent in the direction parallel to the bedding planes of the composite (red) and perpendicular to the bedding planes (blue). In this case, the low-porosity end member is assigned an m value greater than 2, while the high-porosity end member is assigned an m less than 2. Color-coding is the same as in Figure 4.

By analogy with the resistivity index for an isotropic medium

$$I_{\parallel} = \frac{\sigma_{0_{\parallel}}}{\sigma_{t_{\parallel}}} = \frac{\beta\varphi_1^{m_1} + (1-\beta)\varphi_2^{m_2}}{\beta\varphi_1^{m_1}S_{w_1}^{n_1} + (1-\beta)\varphi_2^{m_2}S_{w_2}^{n_2}} \equiv \frac{1}{\bar{S}_w^{n_{\parallel}}} \quad (22)$$

where the definition at the right end of (22) is made by analogy with the corresponding Archie relationship. Similarly

$$I_{\perp} = \frac{\sigma_{0_{\perp}}}{\sigma_{t_{\perp}}} = \frac{\beta\varphi_2^{m_2}S_{w_2}^{n_2} + (1-\beta)\varphi_1^{m_1}S_{w_1}^{n_1}}{\varphi_1^{m_1}S_{w_1}^{n_1}\varphi_2^{m_2}S_{w_2}^{n_2}} \equiv \frac{1}{\bar{S}_w^{n_{\perp}}} \quad (23)$$

where, again, the definition at the right end of (23) is suggested by the analogous Archie relationship. Note that \bar{S}_w is a scalar property while I_{\parallel} , n_{\parallel} , I_{\perp} , and n_{\perp} are all direction-dependent.

ARCHIE'S SATURATION EXPONENT n

Given m_{\parallel} and m_{\perp} , bulk values for n_{\parallel} and n_{\perp} can be solved for. Starting again with equation (1)

$$\sigma_{\parallel} = \beta\sigma_1 + (1-\beta)\sigma_2 \quad (1)$$

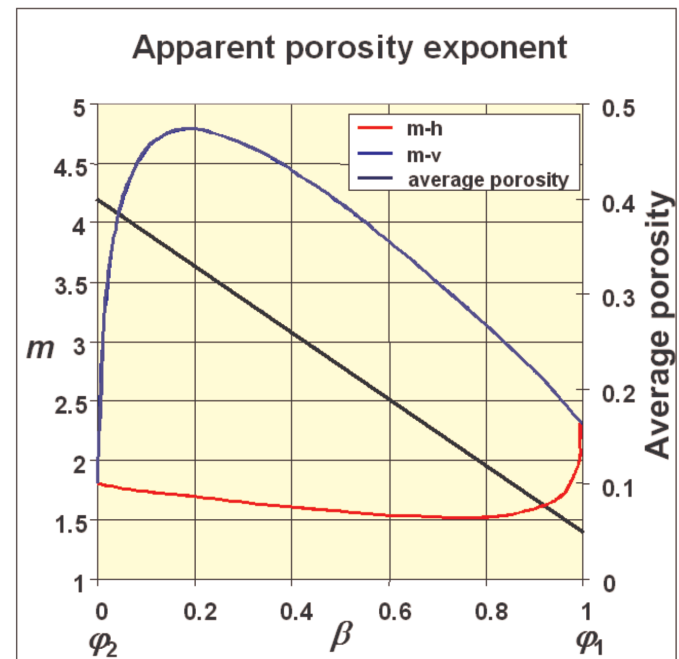


FIG. 7 Another presentation of the variation in Archie porosity exponent with variation in component fraction. The color-coding is the same as in Figure 5.

and substituting the expressions for the conductivities of σ_1 , σ_2 , and σ_{\parallel} results in

$$\sigma_w \bar{\varphi}^{m_1} \bar{S}_w^{n_1} = \beta \sigma_w \varphi_1^{m_1} S_{w_1}^{n_1} + (1 - \beta) \sigma_w \varphi_2^{m_2} S_{w_2}^{n_2}. \quad (24)$$

The solution for n_{\parallel} is

$$n_{\parallel} = \frac{\ln \left(\frac{\beta \varphi_1^{m_1} S_{w_1}^{n_1} + (1 - \beta) \varphi_2^{m_2} S_{w_2}^{n_2}}{\bar{\varphi}^{m_1}} \right)}{\ln \bar{S}_w} \quad (25)$$

Note that σ_1 , σ_2 , m_1 , and m_2 are fixed parameters of the two rock components chosen for the particular model. Similarly S_{w_1} , S_{w_2} , n_1 , and n_2 are likewise fixed for the rock components chosen. S_{w_1} and S_{w_2} are, however, not independent since both are functions of capillary pressure, so a model relating S_{w_1} and S_{w_2} is required to apply this equation. The independent variable in the model actually used is normalized height above "free" water in a reservoir. Otherwise, the only variable is β , the volume fraction of the components.

Similarly for the perpendicular component, beginning with equation (2)

$$\frac{1}{\sigma_{\perp}} = \frac{\beta}{\sigma_1} + \frac{(1 - \beta)}{\sigma_2}, \quad (2)$$

and following the same series of steps that led to equation (24) gives

$$\bar{\varphi}^{m_1} \bar{S}_w^{n_1} = \frac{\varphi_1^{m_1} S_{w_1}^{n_1} \varphi_2^{m_2} S_{w_2}^{n_2}}{\beta \varphi_2^{m_2} S_{w_2}^{n_2} + (1 - \beta) \varphi_1^{m_1} S_{w_1}^{n_1}}. \quad (26)$$

This is easily solved for n_{\perp} ,

$$n_{\perp} = \frac{\ln \left(\frac{1}{\bar{\varphi}^{m_1}} \frac{\varphi_1^{m_1} S_{w_1}^{n_1} \varphi_2^{m_2} S_{w_2}^{n_2}}{\beta \varphi_2^{m_2} S_{w_2}^{n_2} + (1 - \beta) \varphi_1^{m_1} S_{w_1}^{n_1}} \right)}{\ln \bar{S}_w} \quad (27)$$

A MODEL FOR WATER SATURATION AND HEIGHT ABOVE FREE-WATER LEVEL IN THE RESERVOIR

To compute values for n_{\parallel} and n_{\perp} it is necessary to evaluate the water saturations of the two sand fractions in the model at the same height above the free-water level in the reservoir. In other words, a model for the saturation-height function is required. For generality we introduce a function for computing water saturation at each height in the reservoir, expressed in terms of the parameter h/H , where H is the thickness of the hydrocarbon column and h/H is the fractional height above the "free-water level." We use

$$S_w = \begin{cases} 1 & h < h_0 \\ 1 - (1 - S_{w_{irr}}) \left(1 - e^{-\alpha \left(\frac{h}{H} - \frac{h_0}{H} \right)} \right) & h > h_0 \end{cases} \quad (28)$$

to model the "saturation-height" function. In this model $S_{w_{irr}}$ has its usual loosely defined meaning as a pseudo-asymptote. If h_0 is the height above the hydrocarbon-water contact at which hydrocarbon can displace brine from the largest pores in the coarse-grained component, h_0/H corresponds to an "entry" pressure for the component, and α is a "decay constant" that controls the rate at which water saturation diminishes as h/H increases. This function is a qualitative model for observed capillary pressure curves. The sand fractions in the model are assigned different representative values of α , $S_{w_{irr}}$, and h_0/H in order to closely mimic actual capillary pressure data. Making the substitutions

$$S_w = \begin{cases} 1 & h < h_{0_1} \\ 1 - (1 - S_{w_{1irr}}) \left(1 - e^{-\alpha_1 \left(\frac{h}{H} - \frac{h_{0_1}}{H} \right)} \right) & h > h_{0_1} \equiv S_{w_1}(h/H), \end{cases} \quad (28.a)$$

and

$$S_w = \begin{cases} 1 & h < h_{0_2} \\ 1 - (1 - S_{w_{2irr}}) \left(1 - e^{-\alpha_2 \left(\frac{h}{H} - \frac{h_{0_2}}{H} \right)} \right) & h > h_{0_2} \equiv S_{w_2}(h/H) \end{cases} \quad (28.b)$$

effectively changes the variable from two different water saturations to a single value of h/H at any given height in the reservoir. Armed with this model, n_{\parallel} and n_{\perp} can be computed as functions of $0 \leq \beta \leq 1$ and $0 \leq h/H \leq 1$. We emphasize that the function used in (28) is specified for convenience only. Any similar function that may be deemed more "realistic" can be used without changing the effects on the Archie parameters of the composite rock, or the results and conclusions to be drawn therefrom.

Note that I versus S_w has meaning only where $S_w < 1$. The relationship of $S_{w_{1irr}}$ to $S_{w_{2irr}}$ will depend on the saturation-height function for the two components. We consider the usual case where the higher porosity component will typically exhibit a lower water saturation than the lower porosity component. The most succinct notation for expressing the expected relationship is $S_{w_2} \leq S_{w_1} \leq 1$; i.e., the water saturation in the fine-grained (subscript 1), component is greater than, or at most equal to, the water saturation in the coarse-grained (subscript 2), component, and less than, or at most equal to, a fractional volume of 1.0. Accordingly the

domain of n_{\parallel} and n_{\perp} will be taken as, in succinct notation, $h_0/H < h/H < 1$. This is to say that the saturation exponent is not defined, nor even definable, when $S_w = 1.0$ identically.

VARIATION OF n IN A TWO-COMPONENT SANDSTONE

Figure 8 illustrates the saturation-height functions for two sandstone samples. For this plot water saturation is usually presented on the abscissa and height above the hydrocarbon-water contact on the ordinate. The scales in Figure 8 are exchanged to make Figure 9 more readily interpretable. That is, we will plot h/H on the horizontal axis and two functions of water saturation, representing the two sand fractions, on the vertical axis. The diagram illustrates two sands with two different entry pressures, indicated by differing values of h/H , and two different "irreducible" water saturations.

Figure 9 illustrates the relation of the conventional resistivity index plot (shown on the left) and the axes-exchanged saturation-height plot (shown on the right). Since S_w depends upon h/H , the end-member water saturations for the resistivity index plot will vary with h/H , although the

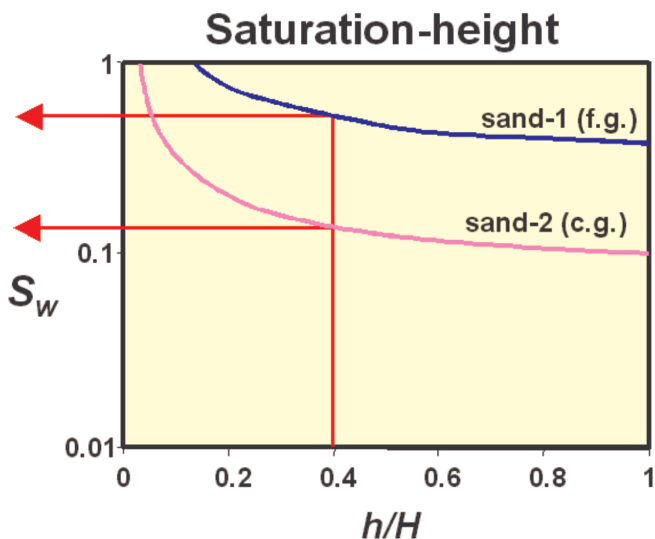


FIG. 8 A saturation-height function, plotted with the conventional axes exchanged. The height function is normalized by the thickness of an oil column measured from the free-water level, plotted on the horizontal axis. Water saturation is plotted on the vertical axis. Note that $S_{w1irr} = 0.40$ for the fine-grained (f.g.) component; $S_{w2irr} = 0.10$ for the coarse-grained (c.g.) component. The illustration shows that for sand components with different capillary pressure curves, the same height above free water h/H in the reservoir corresponds to different water saturations ($S_{w1} = 0.50$; $S_{w2} = 0.10$).

variation may well be small far from the hydrocarbon-water contact. Figure 10 shows the average water saturation as a function of the volume fraction of the components of the

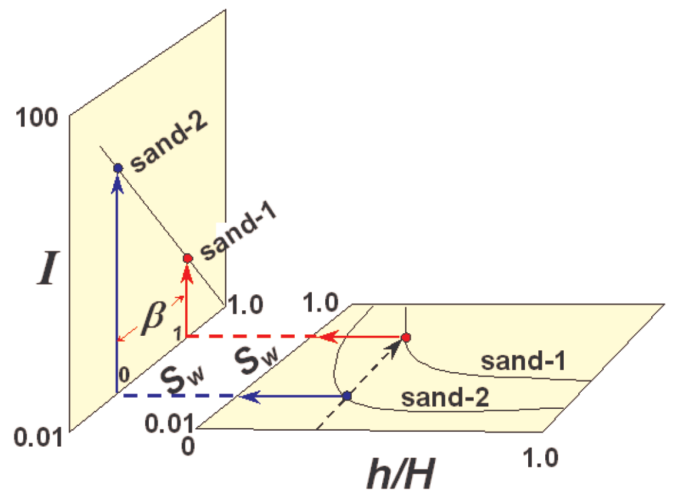
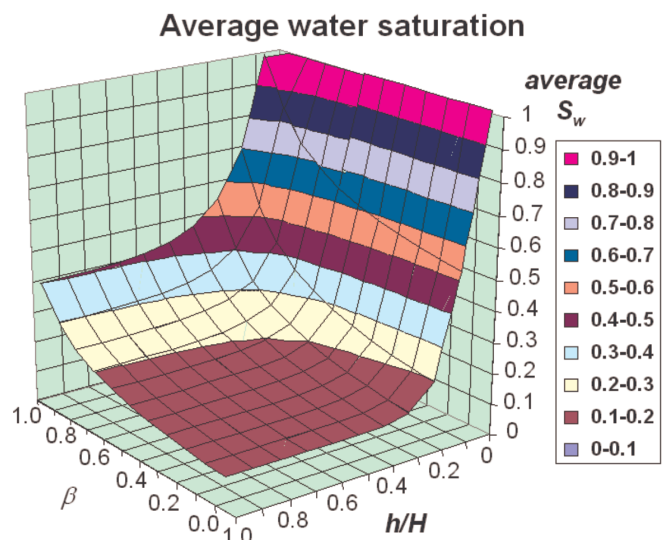


FIG. 9 The resistivity index experiment for a rock composed of two constituents having water saturations (as well as porosities) that differ. The water saturations are coupled through a capillary pressure relationship, and depend upon the height in the reservoir of the samples in question.



$$\bar{S}_w = \frac{\beta\varphi_1 S_{w1} + (1-\beta)\varphi_2 S_{w2}}{\bar{\varphi}} = \frac{\beta\varphi_1 S_{w1} + (1-\beta)\varphi_2 S_{w2}}{\beta\varphi_1 + (1-\beta)\varphi_2}$$

FIG. 10 The average water saturation surface plotted as a function of component fraction and height above free-water level. Notice that the capillary pressure functions of the individual components can be seen in the $\beta = 1$ and $\beta = 0$ planes.

two-component system. Essentially the plot shows that for $\beta = 1$ the saturation-height function is identical to one end member, at $\beta = 0.0$ the saturation-height function is identical to the other end member, and for $0.0 \leq \beta \leq 1.0$ the saturation-height function is a smooth average of the end member component saturation-height functions weighted by the porosity volume fractions of the components.

Figure 11 illustrates four cases of the “parallel” and “perpendicular” resistivity index behavior for sandstone end members having various values of porosity, and porosity and saturation exponents. The figures show clearly that “parallel” saturation exponents $n \approx 1$ are a possible consequence of a rock’s being composited from laminated sandstone fractions (Figures 11a and 11d). Even when *all* the end-member Archie properties (i.e., ϕ , m , n) are approximately equal, the difference in capillary pressure properties is sufficient to induce a strong variation of apparent saturation

exponent as a function of the volume fraction of the components (Figures 11b and 11c).

Figure 11 shows a series of “snapshots” corresponding to a single value of h/H . Figures 12a and 12b are complete representations of n for all values of h/H , as well as all values of the fractional volumes of the components, shown in a representation similar to the presentations of m in Figures 5 and 7. But whereas m depends only upon pore geometry, n depends also upon brine geometry. Obviously, while pore geometry varies with position, it is otherwise a constant property of the rock. However, brine geometry changes as water saturation varies, making the saturation exponent not only a function of position, but also a function of water saturation. The surfaces shown in Figures 12a and 12b bound the volume that contains all the possible values that could be measured for n in the composite medium given the parameters assumed for the end members. The plotting facility did not support the simultaneous plotting of Figures 12a and 12b on the same graph; however, Figure 12b fits atop Figure 12a along the line defined by $n = 2$. In the model of Figure 12, $1.25 < n < 7$ approximately. Since the axes of core plugs are usually selected as close to parallel to the bedding planes as possible, n for core plugs in this rock

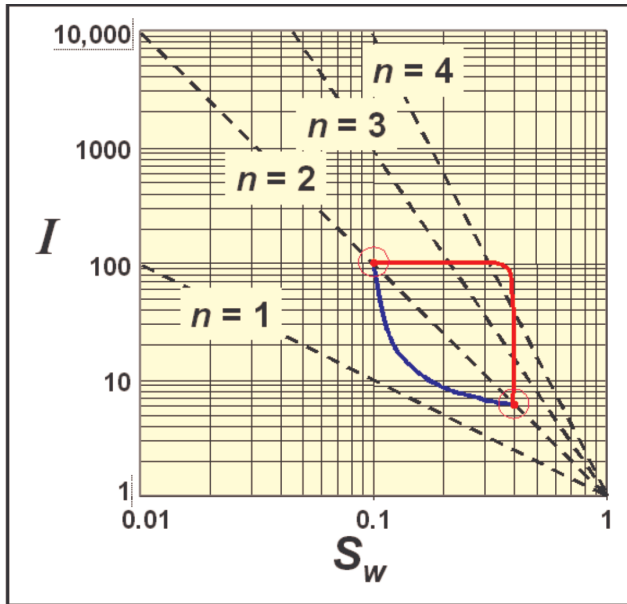


FIG. 11a A resistivity-index–water-saturation plot for a two-component sandstone, analogous to the formation-resistivity factor–porosity plot shown in Figure 4. However, in contrast to the two parameters that vary in Figure 4 (m and ϕ), there are four varying parameters in this case (m , n , ϕ , and S_w). This case illustrates the effects of maximum variation in porosity to be expected in reservoir-quality sandstone, together with the water saturations associated with those components, upon the saturation exponent of the composite. The constituent rocks have identical Archie parameters.

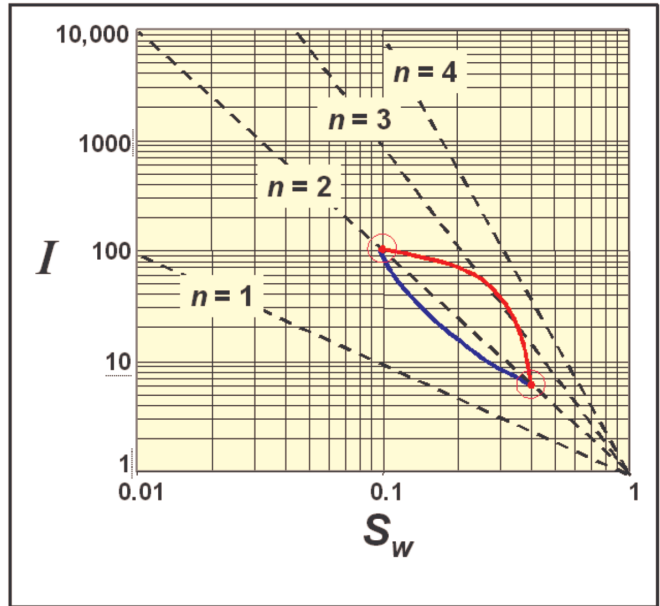


FIG. 11b A plot for a case where all the parameters of the constituent rocks are the same, save for their capillary pressure properties.

would tend to be measured as $1.25 < n < 2.00$ approximately, depending upon the fractional composition and the height above the hydrocarbon-water contact. Figures 12c and 12d show the same surface from a different perspective.

DISCUSSION AND CONCLUSION

Layered media composed from laminations having differing physical properties give rise to anisotropic physical properties at scales larger than the laminations (Maxwell, 1871). Formulas for the conductivity of such composite media are at least 80 years old in the geophysical literature (Schlumberger, 1920). However, only relatively recently have the implications for formation evaluation parameters begun to be recognized (Herrick and Kennedy, 1996). Using the methods of Maxwell and Schlumberger, in this article we have shown that simple laminated rocks composed from layers of locally isotropic, well-behaved sandstones, can exhibit Archie parameters that seem counterintuitive and that are not simple interpolations between the Archie parameters of the component fractions. The fact is that the correct values of the Archie parameters for the composited rocks comprise the components of tensors, and are

not simple volume-weighted averages of the values of the components.

Subsequent to Archie's formulation (1942) of a relationship between formation resistivity and hydrocarbon saturation there followed several decades of vigorous refinement of the understanding of this relationship. However, a thorough consideration of anisotropy appears never to have been an objective of these studies. This lack of concern may have followed from an unexpressed recognition that (in vertical wells) even where anisotropy exists, logging instruments respond directly only to its "horizontal" component, σ_h (ignoring that there might be two different horizontal components, σ_x and σ_y), cores are plugged horizontally when analysis of their Archie parameters is an objective. It was also generally believed that while shales were demonstrably anisotropic, sands should be isotropic, at least approximately. Horizontal drilling and logging have shown such a view of reservoir rocks to be too simple, and it is a current industry goal to understand the effects of anisotropy both on logging instrument responses and also on the industry-standard techniques of formation evaluation. The effects reported upon herein have indicated that there is a

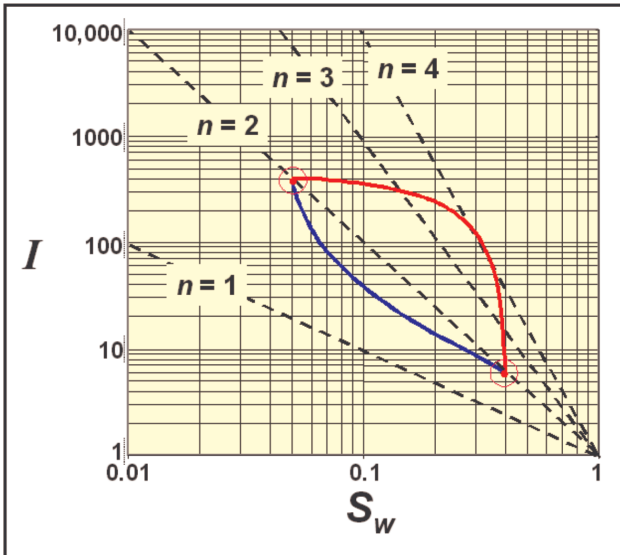


FIG. 11c A plot for a case where all the parameters of the constituent rocks are the same as in Figure 11b, except that the irreducible water saturation of the high-porosity component is reduced by 5 s.u.

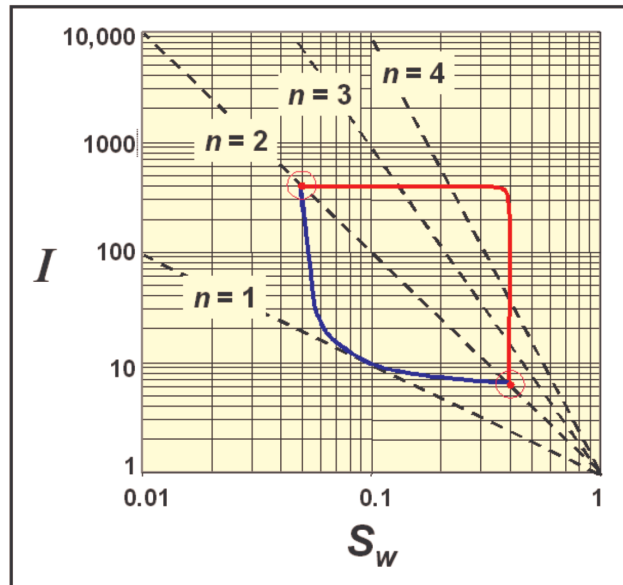


FIG. 11d Plot for a case where all the parameters of the constituent rocks are the same as in Figure 11a, except that the porosity exponents of the end members are assigned the "more realistic" values used in Figure 3.

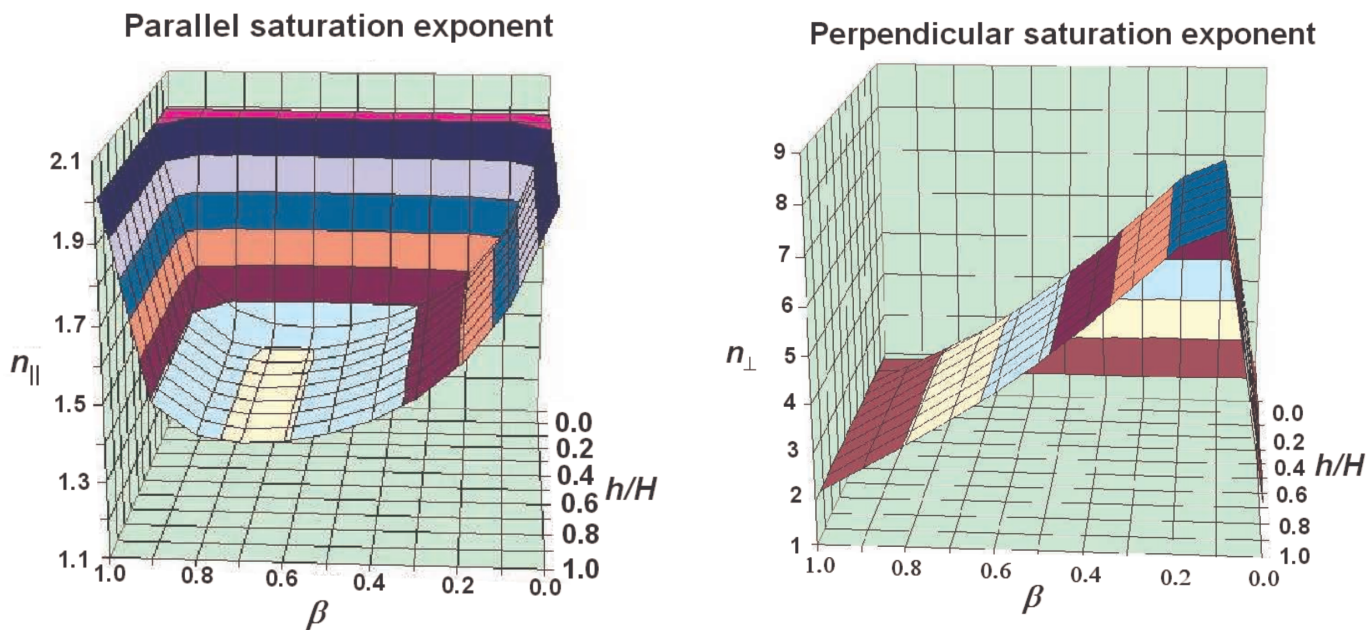


FIG. 12a The Archie saturation exponent for the composite medium measured in a direction parallel to bedding planes between the components of the composite. If one of the components retains a high water saturation while the other has most of its water displaced by hydrocarbons, the composite medium can have low saturation exponent values, once thought to be anomalous, but shown here to follow directly from the properties of the medium.

FIG. 12b The Archie saturation exponent for the composite medium measured in a direction perpendicular to bedding planes between the components of the composite. If one of the components retains a high water saturation while the other has most of its water displaced by hydrocarbons, the composite medium can have high saturation exponent values, once thought to be anomalous, but shown here to follow directly from the properties of the medium.

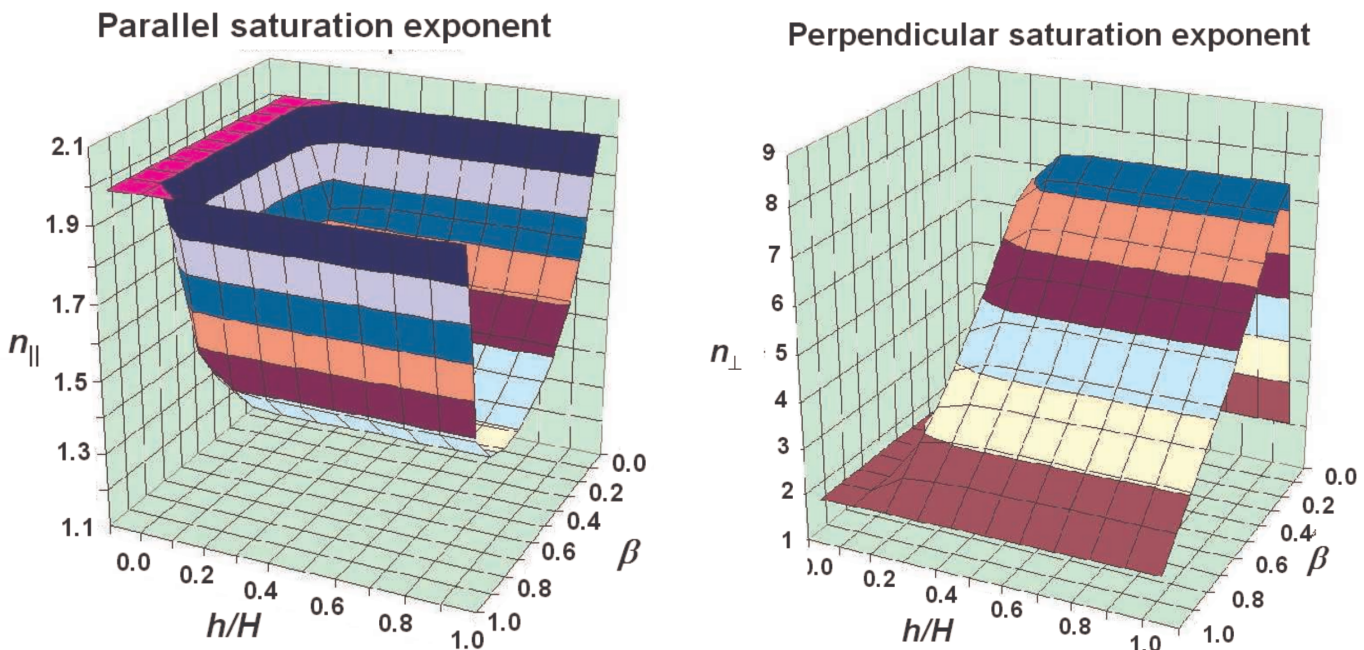


FIG. 12c The same boundary illustrated in Figure 12a, but shown from a different perspective.

FIG. 12d The same bounding surface illustrated in Figure 12b, but shown from a different perspective.

definite effect in layered rocks. Since all clastic rocks are layered to a greater or lesser degree, evidence of these effects has doubtless been observed but has gone unremarked upon.

The practicality of these results depends upon whether the effects are significant, not for end members selected to have extreme property values for theoretical purposes, but for ensembles of rocks encountered in actual petroleum reservoirs observed using standard techniques. The resistivity index experiment—covering, as it does, all water saturations from $S_w = 1.0$ down to S_{wirr} —naturally observes the entire range of the S_w parameter from one saturation end member to the other. The variation in n_{\parallel} predicted by the two-component model is totally supported by observations in rocks (LaTorra and Hall, 1991).

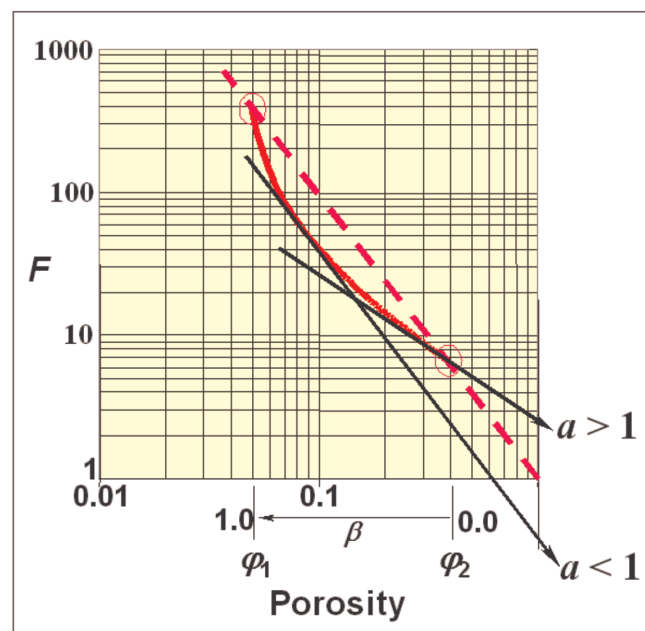
On the other hand, porosity variations in real reservoirs are typically less than the extremes that we have used as limiting-case end members. What will be the effect of taking variation more typical of actual reservoirs? Let us first recognize that if the pure porosity end members of the composite are never observed because they do not occur in quantities thick enough to be sampled as “homogeneous” plugs, then the porosity variation observed in a laboratory will be less than the porosity variation between the actual end members in the reservoir. In other words, it is possible that the scale of our observations is too coarse to sample the porosity variation that actually exists. In this situation, the fact that bulk porosity is observed to vary over a certain range is not equivalent to a statement regarding the variation between the true end members of the composite, which will be larger. To identify this condition core plugs would have to be examined on a scale as small as the visible laminations in the plugs. We are not arguing that every reservoir, or any reservoir, has actual porosity end members near 5 porosity units (p.u.) and 40 p.u. We are saying that the mere fact that porosity varies between two “apparent” limiting values in a certain suite of observations on core plugs should not necessarily be interpreted as the observed porosity values representing the porosity end member values in those plugs.

There should be observable consequences of a limited observable β range. Recall that the formation resistivity factor is often defined as $F = a/\phi''$, where a is the “intercept” of a line least squares-fitted to observed formation-resistivity factor–porosity data with the vertical axis crossing the horizontal axis at 100 porosity units. For example, in the well known “Humble” formula, $a = 0.62$, $m = 2.15$ (Winsauer et al., 1952). Specifically, $a < 1$ for the Humble formula. For other data sets $a > 1$. Figure 13 illustrates that for a case where the reservoir is laminated with typically low β (higher porosity), a line fit through data collected at random in such a reservoir will exhibit $a > 1$. Conversely, for a res-

ervoir with typically high β values (lower porosity), $a < 1$. Thus, use of conductivity anisotropy theory explains the origin of intercepts $a \neq 1$ in terms of sand lamination volume fraction distribution. We are not claiming that effects of anisotropy and skewed volume fraction distribution of conductive sand components in laminated reservoirs are the sole causes for $a \neq 1$, but we suggest that anisotropy is at least one previously unrecognized cause.

Figure 14 illustrates the effect on porosity exponents of a smaller range of porosity variation in the end members. In this figure we introduce approximate values of m that would be measured on core plugs inclined at angles oblique to parallel and perpendicular orientations of the core plug. The computations leading to these curves are explained in Appendix B. Not surprisingly, the variation in m diminishes as the properties of the end members tend toward equality.

Formation resistivity factors of layered media



$$\begin{aligned} \varphi_1 &= 0.05, & m_1 &= 2.0 \\ \varphi_2 &= 0.40, & m_2 &= 2.0 \end{aligned}$$

FIG. 13 The figure illustrates the effect of a limited range of porosity variation in a laminated reservoir. If the high-porosity end member predominates, a least-squares fit of a line to the data will have an intercept $a > 1$. Conversely, if the low-porosity end member predominates, then the least-squares line will have $a < 1$. These possibilities arising in a laminated sand reservoir suggest a physical cause for observations where $a \neq 1$.

Obviously the effect would vanish for end members chosen to have the same porosity and the same Archie exponent for they would then be electrically identical.

A study of many cases (not shown) reveals that the details of the porosity exponent function depend not only upon the separation in porosity units but also upon where the end members are located on the porosity axis. The effects of laminations are likely to be a consistently smaller source of uncertainty in m than in n , especially if the core plug axes are substantially parallel to the planes bounding the laminations. However, in formation analysis a conscious and explicit choice of whether to ignore, or to attempt to account for, anisotropy effects on log responses and parameter selection should be made on a case by case basis.

This analysis has shown that small errors in orientation of core plugs lead to correspondingly small errors in the determination of m values in special core analysis. The

close analogy of the relations of F to m and I to n suggests that if $m \approx m_{\parallel}$ for small departures of the core plug axis from parallel to laminations, then $n \approx n_{\parallel}$ should also be true. The analysis has likewise shown that a large amount of variation in these values, depending on the volume fraction of the constituent components, is legitimate. This variation has gone largely unexplained in the past, or else has been attributed to measurement error in special core analysis.

The first representatives of tri-axial induction logging instruments capable of separately resolving the components of the conductivity tensor are now being employed in the field. Whereas formation resistivity was previously considered to be a single number, using these instruments it will be resolved into two (R_{\parallel}, R_{\perp}), or even three (R_x, R_y, R_z) numbers at each point in the formation. Thus, the implications for formation evaluation of the variation in Archie's parameters m and n (or, we should perhaps say "Archie's tensors \hat{m} and \hat{n} ") with the composition and orientation of sand laminations—or indeed, whether there are *any* unrecognized implications—clearly needs to be evaluated. Such an evaluation is the next step in understanding and quantifying the electrical behavior of reservoir rocks, as used in formation evaluation, as thoroughly as possible.

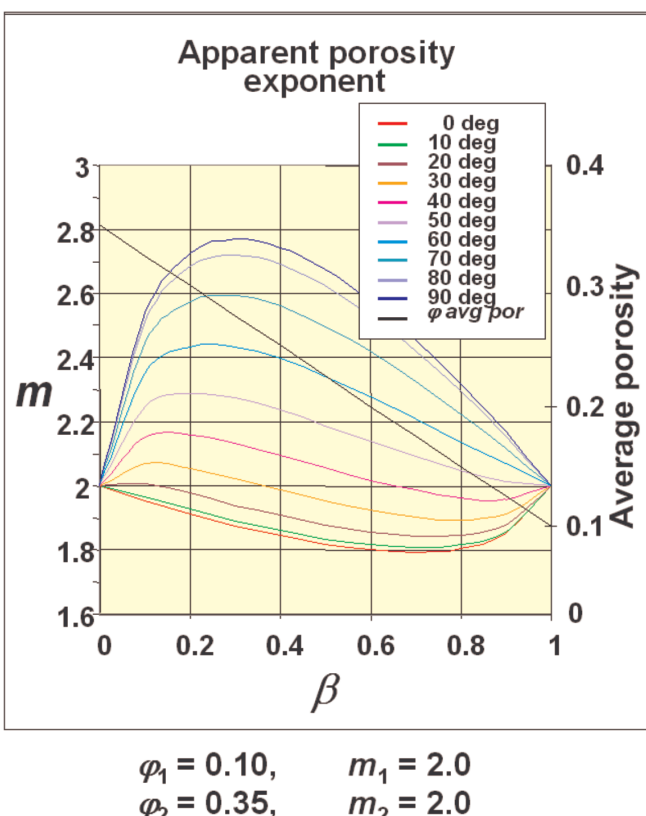


FIG. 14a The effect of constituent end-member porosities on composite porosity exponent values. The end member porosities used to develop the theory of Archie's parameters in a laminated, composite medium were at the extremes of the possible variations in porosity. In this figure a diminishing of the effect is recorded as end member porosities are chosen to lie more closely together. Archie's original data from the Nacatosh sandstone exhibits a variation of approximately $0.10 < \phi < 0.35$.

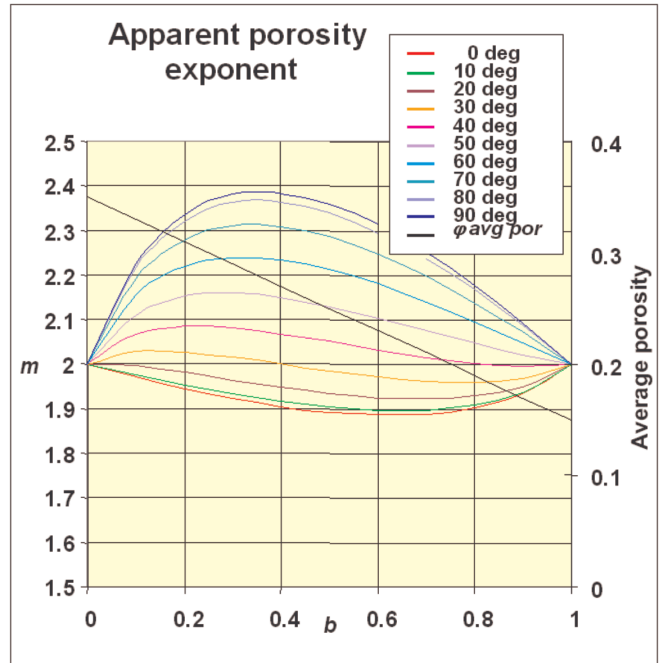


FIG. 14b The effect of constituent end-member porosities on composite porosity exponent values. With end members separated by 20 p.u.s the dispersion of m is less pronounced, but might still be significant for formation evaluation if the rock has a value of $\beta = 0.6$ and a value of $m = 2$ is used in formation evaluation, rather than the correct value of $m = 1.9$.

Also of note is a feature of the use of power laws in the description of the relationships connecting formation resistivity factors and porosity, and resistivity index and water saturation. As we have calculated them for this article, the values of m_{\parallel} and m_{\perp} at a point in the $\log \varphi$ - $\log F$ plane is the slope of a line connecting that point with $(\varphi = 1, F = 1)$ having a formula of the form $m = -\log F/\log \varphi$. As suggested by Figures 3 and 13, if the $\log \varphi$ - $\log F$ function is not a power law containing the point (1,1), the slope of its graph would be better defined as $m = d(\log F)/d(\log \varphi)$. The latter (re)definition would require a lengthy study and explanation of its consequences. Such a study is beyond the scope of this research, and although the numerical values of m (and n) would be changed by such a redefinition, the fundamental conclusions of this study regarding the genesis of anisotropy in shale-free sand would remain unchanged. It is interesting to note that Winsauer's (1952) method implicitly finds a line that is parallel to a tangent to a curve that could be imagined to describe the trajectory of a data set in $\log \varphi$ - $\log F$ space.

We close this article with a remark on the generality of these results. The use of a two-component composite in this

study is engendered solely by its being the simplest non-trivial case. Clearly real composites can be, and are, multi-componented. The two-component analysis readily generalizes. The generalized multicomponent formulation of this analysis is given in Appendix C.

ACKNOWLEDGMENTS

Our colleague Tom Barber encouraged the early development of this work. Suggestions for enhancement of the content of this article offered by Drs. Hezhu Yin, Dale Fitz, Quinn Passey, Karen Love, and other ExxonMobil colleagues are greatly appreciated and contributed to making this a more thorough and readable article. The anonymous reviewers and the associate editor also provided valuable guidance. We are, of course, grateful to ExxonMobil and BakerHughes for permission to communicate these findings to the greater petrophysics community, and especially to our immediate supervisors who sponsored the considerable expense for color in the figures.

REFERENCES

- Archie, G. E., 1942, The electrical resistivity log as an aid in determining some reservoir characteristics: *Petroleum Technology*, vol. 5, no. 1, T.P. 1422, 8 p.
- Herrick, D. C. and Kennedy, W. D., 1996, Electrical properties of rocks: Effects of secondary porosity, laminations, and thin beds, paper C, in 37th Annual Symposium SPWLA Transactions: Society of Professional Well Log Analysts.
- Kennedy, W. D., Herrick, D. C., and Yao, T., 2001, Calculating Water saturation in electrically anisotropic media: *Petrophysics*, vol. 42, no. 2, p. 118–136.
- LaTorra, G. A. and Hall, C. G., 1991, Observations of rock fabric controls on the electrical properties of sandstones, Paper 9116, in SCA Conference Transactions: Society of Core Analysts.
- Maxwell, James C., 1871, in *A Treatise on Electricity and Magnetism*, Volume I (Third Edition, Preface by J. J. Thompson) in the section “On Stratified Conductors,” article 321 appearing on page 446.
- Schlumberger, C., 1920, Etude sur la prospection électrique du sous-sol, Paris, Gauthier-Villars, p. 40.
- Winsauer, W. O., Shearin, H. M., Jr., Masson, P. H., and Williams, M., 1952, Resistivity of brine-saturated sands in relation to pore geometry: *AAPG Bulletin*, vol. 38, no. 2, p. 253–277.

NOMENCLATURE

β	fractional volume of the “first” component (taken as fine grained)
$1 - \beta$	fractional volume of the “second” component (taken as coarse grained)
$\alpha; \alpha_1; \alpha_2$	curvature parameter for saturation-height functions

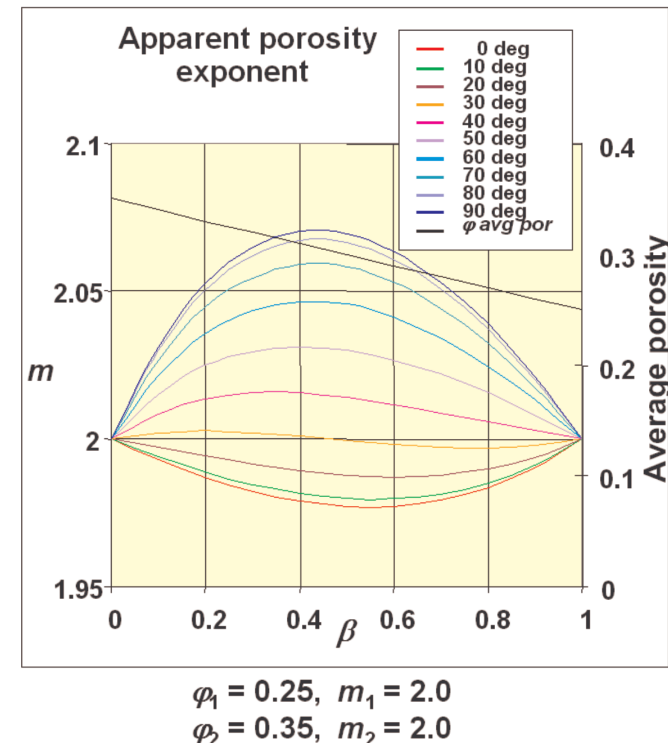


FIG. 14c The effect of constituent end-member porosities on composite porosity exponent values. With end members separated by 10 p.u.s the dispersion of m is probably less than the uncertainty in the determination of m in most cases.

δ	relative deviation, angle between the z -coordinate axis and the σ_{\perp} axis	$R_{\parallel}; R_{\perp}$	resistivity components parallel/perpendicular to bedding
$\hat{\mathbf{R}}; \hat{\mathbf{R}}^T$	left and right components of a similarity transform	H	reservoir thickness
ψ	angle between applied electric field \mathbf{E} and induced current density \mathbf{J}	h	height above “free-water” level in a reservoir
a	intercept parameter in the Humble formula	h_0	height at which entry pressure is exceeded for a reservoir component
$m; m_1; m_2$	Archie’s porosity exponent in the first and second components	$h_{01}; h_{02}$	h_0 in the first and second components
$m_{\parallel}; m_{\perp}$	m component parallel to bedding;	H	thickness of hydrocarbon column in a reservoir
	m component perpendicular to bedding		
$n; n_1; n_2$	Archie’s saturation exponent in the first and second components	h/H	“fractional” height above “free water” in the reservoir
$n_{\parallel}; n_{\perp}$	n component parallel to bedding;		
	n component perpendicular to bedding		
$\hat{\mathbf{m}}; \hat{\mathbf{n}}$	porosity exponent and saturation exponent tensors, respectively		
$\hat{\mathbf{m}}_D; \hat{\mathbf{n}}_D$	porosity and saturation exponent tensors in their diagonal forms		
$S_w; \bar{S}_w$	water saturation and volume-weighted average water saturation		
$\bar{S}_{w_1}; \bar{S}_{w_2}$	water saturation in the first and second components		
$\bar{S}_{w_{1irr}}; \bar{S}_{w_{2irr}}$	“irreducible” water saturation in the first and second components		
$\varphi; \bar{\varphi}$	porosity and volume-weighted average porosity		
$\varphi_1; \bar{\varphi}_2$	porosity in the first and second components		
S_w	volume fraction of brine in a formation		
φS_w	volume-weighted average fraction of brine in a multicomponent formation		
$F; F_1; F_2$	formation resistivity factor in the first and second components		
$F_{\parallel}; F_{\perp}$	formation resistivity factor component parallel or perpendicular to bedding		
$I; I_1; I_2$	resistivity index in the first and second components		
$I_{\parallel}; I_{\perp}$	resistivity index component parallel or perpendicular to bedding		
$\sigma_w; R_w$	brine conductivity; resistivity		
$\sigma_t; R_t$	hydrocarbon-bearing formation conductivity or resistivity parallel to bedding planes		
$\sigma_{0\parallel}; R_{0\parallel}$	water-bearing formation conductivity or resistivity parallel to bedding planes		
$\sigma_1; \sigma_2$	isotropic conductivity in the first and second components		
$\sigma_h; \sigma_v$	bulk horizontal or vertical conductivity components		
$\sigma_{\parallel}; \sigma_{\perp}$	conductivity components parallel/perpendicular to bedding		

APPENDIX A: DEFINITIONS

Average porosity $\bar{\varphi}$ and water saturation \bar{S}_w are well-defined physically. Likewise, the experiments to determine the formation resistivity factors parallel and perpendicular to bedding planes are quite definite, easily performed, and have easily understood results. Therefore, Archie’s relations can be used to define exponents that apply in a fashion analogous to Archie’s relations in isotropic media. That is

$$\begin{aligned} F_{\parallel} &\equiv 1/\bar{\varphi}^{m_{\parallel}} & I_{\parallel} &\equiv 1/\bar{S}_w^{n_{\parallel}} \\ F_{\perp} &\equiv 1/\bar{\varphi}^{m_{\perp}} & I_{\perp} &\equiv 1/\bar{S}_w^{n_{\perp}} \end{aligned}$$

are the *definitions* of m_{\parallel} , m_{\perp} , n_{\parallel} , and n_{\perp} .

APPENDIX B: APPLICATION TO TENSOR ARCHIE THEORY

Kennedy et al. (2001) showed that Archie’s law for isotropic rocks generalizes into the form

$$\hat{\sigma}_t = \sigma_w \varphi^{\hat{\mathbf{m}}} S_w^{\hat{\mathbf{n}}} \quad (\text{B.1})$$

where the conductivity tensor on the left, $\hat{\sigma}_t$, is reflected on the right side by the “porosity” tensor $\varphi^{\hat{\mathbf{m}}}$ and the “saturation” tensor $S_w^{\hat{\mathbf{n}}}$. Note that φ and S_w themselves are scalars, but raised to the matrix powers the resulting quantities are tensors. We could guess that $\varphi^{\hat{\mathbf{m}}}$ and $S_w^{\hat{\mathbf{n}}}$ are tensor quantities simply because the left-hand side of (B.1) is a tensor, thereby requiring whatever is on the right side to also be a tensor quantity. Tensors are distinguished from other matrices by their properties under coordinate transformations and it can be shown by means of such transformations that $\hat{\mathbf{m}}$ and $\hat{\mathbf{n}}$ are themselves tensors in their own right. Kennedy et al. contemplated that the principal components of the conductivity tensor would be available through laboratory measurements, and we have shown that for transversely isotropic media comprised of locally isotropic, laminated sands, the principal components can be theoretically pre-

dicted if the volume fraction and Archie parameters of the individual components are known. Thus

$$\hat{\mathbf{m}}_D = \begin{bmatrix} m_{\parallel} & 0 & 0 \\ 0 & m_{\parallel} & 0 \\ 0 & 0 & m_{\perp} \end{bmatrix}, \quad \hat{\mathbf{n}}_D = \begin{bmatrix} n_{\parallel} & 0 & 0 \\ 0 & n_{\parallel} & 0 \\ 0 & 0 & n_{\perp} \end{bmatrix}, \quad (\text{B.2})$$

where m_{\parallel} , m_{\perp} , n_{\parallel} , and n_{\perp} are given by the formulas developed in the text for a two-component system, or developed in Appendix C for a multicomponent system.

These tensor components are functions of the fractional volumes of the constituents, and indicate the results of experiments parallel and perpendicular to bedding planes, but it is natural to question what effect the orientation might have if the measurements are skewed with respect to these directions. Is the effect large or small?

One way to approximate an answer is graphically. For example, in Figure 5 the red line represents measurements taken at 0° with respect to the bedding planes, while the blue line represents measurements taken at 90° with respect to the bedding planes. Obviously, measurements at intermediate angles would be expected to be intermediate in some fashion. So a grid of parameter lines at 10° , 20° , ..., 80° could be sketched between the red and blue lines using some interpolation scheme. The only physics applied would be an assumption that the function of angle, whatever it may be, is smoothly varying. On the other hand, the problem is somewhat, if not entirely, amenable to a theoretical analysis.

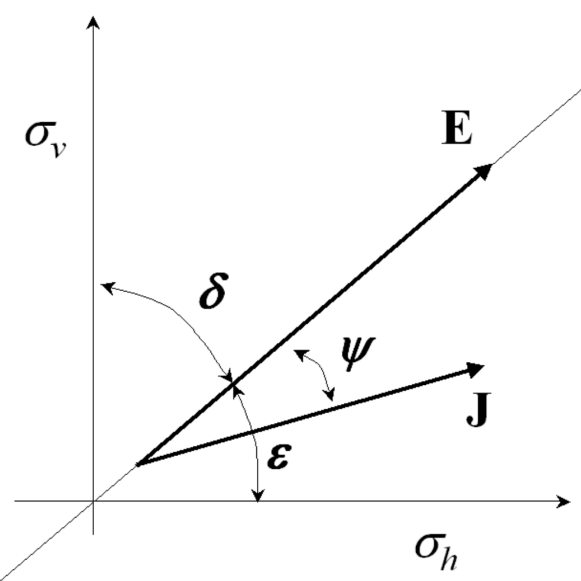


FIG. B.1a The relation of the current density vector \mathbf{J} to the applied electric field \mathbf{E} in an unbounded transversely isotropic medium.

In unbounded media the component of the Archie parameters in various directions could be obtained directly from the principal component forms (i.e., equations (B.2) and their tensor properties. Thus at a relative deviation of δ

$$\hat{\mathbf{m}} = \hat{\mathbf{R}} \hat{\mathbf{m}}_D \hat{\mathbf{R}}^T = \begin{bmatrix} m_{xx} & m_{xy} & m_{xz} \\ m_{yx} & m_{yy} & m_{yz} \\ m_{zx} & m_{zy} & m_{zz} \end{bmatrix} \quad (\text{B.3})$$

where $\hat{\mathbf{R}}^T$ is the transpose of $\hat{\mathbf{R}}$ and

$$\hat{\mathbf{R}}(\delta) = \begin{bmatrix} \cos \delta & 0 & -\sin \delta \\ 0 & 1 & 0 \\ \sin \delta & 0 & \cos \delta \end{bmatrix}, \quad (\text{B.4})$$

and a similar expression would hold for $\hat{\mathbf{n}}$. Unfortunately, in the laboratory things are not so simple.

Figure B.1a illustrates that in the unbounded medium there is no doubt that the current density \mathbf{J} has a component parallel $J_{\parallel E}$ (J parallel to E) to, and a component perpendicular $J_{\perp E}$ (J perpendicular to E) to, the applied electric field \mathbf{E} ; i.e., linear superposition holds for the current density field. However, as Figure B.1b illustrates, the $J_{\perp E}$ component is constrained by the physical boundary of a core plug. Since the current density component perpendicular to the applied field cannot circulate, as suggested in Figure B.2

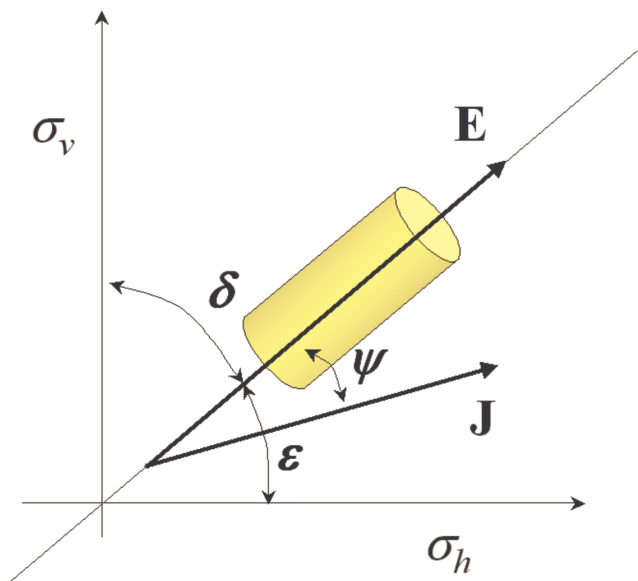


FIG. B.1b Current density in a core plug. Here the current density cannot develop as it would in an unbounded medium. Neglecting end effects, what would the resulting current density, and the associated conductivity, be? And how would it be related to the conductivity tensor components?

only the $J_{||E}$ component is non-zero, and the effective conductivity of the medium is given by the ratio $J_{||E}/|E|$. This pretty picture is spoiled by end effects that are not amenable to elementary analysis. We believe such effects will be small for core plugs with a large aspect ratio; i.e., for “long” plugs. End effects could not be neglected for short plugs, and for plugs having an aspect ratio near unity a resort to numerical methods would be necessary to determine the magnitude of the current traversing the plug.

The case of the “long” core plug is susceptible to analysis. Consider a hypothetical medium, of the kind we have been discussing, composed of two components. The medium is therefore anisotropic at a scale larger than its layer thicknesses. We want to consider two core plugs cut parallel and perpendicular to the tensor principal axes, and a set cut every one degree between the parallel (call

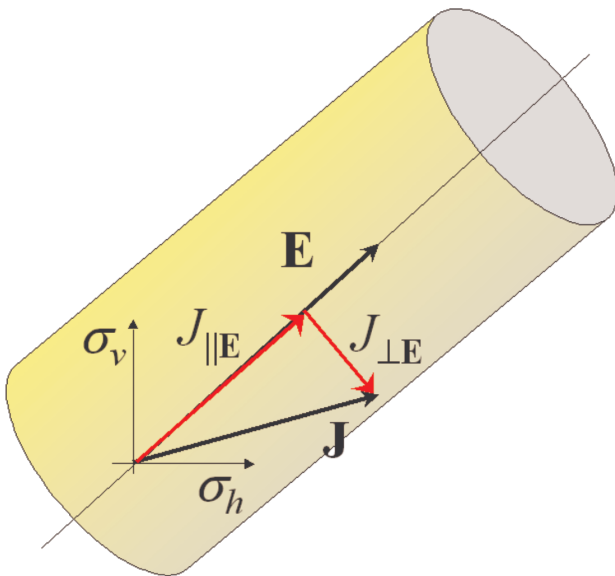


FIG. B.2 Development of apparent conductivity in a misaligned core plug. In the unbounded medium there is no doubt that the current density \mathbf{J} has components parallel ($J_{||E}$) and perpendicular ($J_{\perp E}$) to the applied electric field \mathbf{E} ; i.e., linear superposition holds for the current density field. However, the $J_{\perp E}$ component is constrained by the physical boundary of a core plug. Since the current density component perpendicular to the applied field cannot circulate, only the $J_{||E}$ component is non-zero, and the effective conductivity of the medium is given by the ratio $J_{||E}/|E|$. This pretty picture is spoiled by end effects that are not amenable to easy analysis. I believe such effects will be small for core plugs with a large aspect ratio. End effects could not be neglected for short plugs, and for plugs having an aspect ratio near unity a resort to numerical methods would be necessary to determine the magnitude of the current traversing the plug, and consequently m and n .

this x -directed) and the perpendicular (call this z -directed) principal components. To each of these samples we propose to apply an electric field of 1 volt per meter. For the sample cut at an angle δ with respect to the horizontal principal axis, the electric field components are $E_x = \cos \delta$ and $E_z = \sin \delta$. The current density components are then $J_x = \sigma_x E_x = \sigma_x \cos \delta$ and $J_z = \sigma_z E_z = \sigma_z \sin \delta$. In general, because the medium is anisotropic, this current density vector \mathbf{J} is not parallel to the applied electric field \mathbf{E} . The angle ψ between \mathbf{J} and \mathbf{E} is given from elementary vector analysis as

$$\cos \psi = \frac{\mathbf{E} \cdot \mathbf{J}}{|\mathbf{E}| |\mathbf{J}|} = \frac{\sigma_x E_x^2 + \sigma_z E_z^2}{\sqrt{E_x^2 + E_z^2} \sqrt{(\sigma_x E_x)^2 + (\sigma_z E_z)^2}}. \quad (\text{B.5})$$

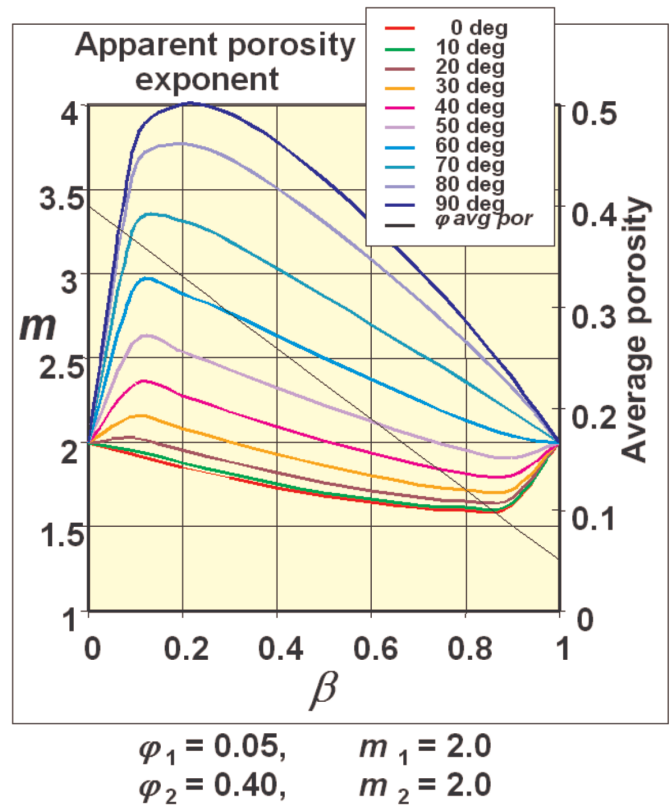


FIG. B.3 Variation of the porosity exponent as a function of alignment of the sample. If the value of the porosity exponent depends upon the relative fractional volumes of the constituents and whether the measurements are performed parallel to, or perpendicular to, the bedding planes, what is the effect of a misalignment of the core plug axis? The chart suggests that small misalignments (less than 10 degrees) will induce correspondingly small errors. The curves on this chart are not universally applicable but depend upon a number of assumptions explained in the text. The parameters in this model are the same as those used in Figure 5.

The current that can flow through the core plug that we are considering is constrained to flow parallel to the plug axis. This will be the component of current density that is parallel to \mathbf{E} . This component is just the projection of \mathbf{J} onto \mathbf{E} given by $J_{\parallel E} = |\mathbf{J}| \cos \psi$. Given that $|\mathbf{E}| = 1$, the result is simply $J_{\parallel E} = \sigma_x \cos^2 \psi + \sigma_z \sin^2 \psi$.

From Ohm's law in field theory form, namely, $\mathbf{J} = \hat{\sigma} \mathbf{E}$, we assert that $\sigma_{\parallel E} = J_{\parallel E} / |\mathbf{E}| = J_{\parallel E}$, since $|\mathbf{E}| = 1$ by design. By an extension of Archie's definition $\sigma_{\parallel E} = \sigma_w \bar{\varphi}^{m_{\parallel E}}$. This can be solved for $m_{\parallel E}$ resulting in

$$m_{\parallel E} = \frac{\ln \sigma_{\parallel E}}{\ln \bar{\varphi}} \quad (\text{B.6})$$

Now $m_{\parallel E} = m_{\parallel E}(\beta, \delta)$, depending upon β through the conductivity and average porosity, and upon δ through the angle that the axis of the core plug makes with the planes of lamination. This is the formula that we used to compute the approximate parameter curves in Figure B.3. The parameters are exact in the limit of a very long core plug, otherwise they are approximate. Their direct connection to the physics of this problem makes them a more useful heuristic device than a mere interpolation would have provided. For example, it can be seen in Figure B.3 that the line at 10° from the horizontal is essentially not distinguishable from the horizontal parameter line itself. This means that slight errors in choosing the direction of a plug axis will have a negligible effect on measurements made on the core.

A similar, albeit more complicated, analysis would yield the $n_{\parallel E}$ surfaces that would partition the volume bounded by n_{\parallel} and n_{\perp} shown in Figures 12.

APPENDIX C: MULTICOMPONENT SANDSTONE COMPOSITE THEORY

The two-component model developed in the text is the simplest nontrivial special case of a multicomponent model. It is not hard to formulate the model in terms of any number of components.

For an anisotropic medium comprising laminated, locally isotropic media characterized in the i th layer by $\sigma_i = \sigma_w \varphi_i^{m_i} S_{w_i}^{n_i}$, the bulk petrophysical properties can be characterized in terms of the individual layer properties and the specific volumes of the layer types. The specific volume V_i of the i th component layer is the ratio of the thickness of the i th layer to the thickness of the section. For a system of k components, the volumes must be conserved, so

$$\sum_{i=1}^k V_i = 1. \quad (\text{C.1})$$

The volume-weighted average porosity is

$$\bar{\varphi} = \sum_{i=1}^k V_i \varphi_i, \quad (\text{C.2})$$

and the volume-weighted water fraction is

$$\overline{\varphi S_w} = \sum_{i=1}^k V_i \varphi_i S_{w_i}, \quad (\text{C.3})$$

leading to the average water saturation for the composite

$$\bar{S}_w = \frac{\overline{\varphi S_w}}{\bar{\varphi}} = \frac{\sum_{i=1}^k V_i \varphi_i S_{w_i}}{\sum_{i=1}^k V_i \varphi_i}. \quad (\text{C.4})$$

The volume-weighted average conductivity parallel to the bedding planes is

$$\bar{\sigma}_{\parallel} = \sum_{i=1}^k V_i \sigma_i = \sum_{i=1}^k V_i \sigma_w \varphi_i S_{w_i}^{n_i} = \sigma_w \sum_{i=1}^k V_i \varphi_i S_{w_i}^{n_i} \quad (\text{C.5})$$

and the generalized Archie relation is simply

$$\bar{\sigma}_{\parallel} = \sigma_w \bar{\varphi}^{m_{\parallel}} S_w^{n_{\parallel}}. \quad (\text{C.6})$$

This relationship defines m_{\parallel} and n_{\parallel} . The generalized porosity exponent is then obtained by evaluating the function at $S_w = 1.0$, and using the definition in (C.6). That is

$$\bar{\sigma}_{\parallel} \Big|_{S_w=1} = \sigma_w \bar{\varphi}^{m_{\parallel}} = \sigma_w \sum_{i=1}^k V_i \varphi_i^{m_i} \quad (\text{C.7})$$

The result is

$$m_{\parallel} = \frac{\ln \sum_{i=1}^k V_i \varphi_i^{m_i}}{\ln \sum_{i=1}^k V_i \varphi_i} \quad (\text{C.8})$$

Then knowing m_{\parallel} , n_{\parallel} can be evaluated as

$$n_{\parallel} = \frac{\ln (\sum_{i=1}^k V_i \varphi_i^{m_i} S_{w_i}^{n_i} / \bar{\varphi}^{m_{\parallel}})}{\ln \bar{S}_w}. \quad (\text{C.9})$$

The generalized Archie exponents for the direction perpendicular to bedding are similarly developed leading to formulas only slightly more complicated. The volume-weighted average conductivity perpendicular to bedding planes is

$$\frac{1}{\sigma_{\perp}} = \sum_{i=1}^k \frac{V_i}{\sigma_i} = \sum_{i=1}^k \frac{V_i}{\sigma_w \varphi_i^{m_i} S_{w_i}^{n_i}} = \frac{1}{\sigma_w} \sum_{i=1}^k \frac{V_i}{\varphi_i^{m_i} S_{w_i}^{n_i}} \quad (\text{C.10})$$

and the relation

$$\bar{\sigma}_\perp = \sigma_w \bar{\varphi}^{m_\perp} S_w^{n_\perp}. \quad (\text{C.11})$$

provides a definition for m_\perp and n_\perp . Evaluating at $S_w = 1$ gives

$$\bar{\sigma}_\perp|_{S_w=1} = \sigma_w \bar{\varphi}^{m_\perp}. \quad (\text{C.12})$$

then

$$\frac{1}{\bar{\varphi}^{m_\perp}} = \sum_{i=1}^k \frac{V_i}{\varphi^{m_i}} \Rightarrow \bar{\varphi}^{m_\perp} = 1 / \sum_{i=1}^k \frac{V_i}{\varphi^{m_i}} \quad (\text{C.13})$$

and finally

$$m_\perp = - \frac{\ln \sum_{i=1}^k V_i / \varphi^{m_i}}{\ln \bar{\varphi}}. \quad (\text{C.14})$$

Once m_\perp is known, n_\perp can be found by

$$\frac{1}{\varphi^{m_\perp} \bar{S}_w^{n_\perp}} = \sum_{i=1}^k \frac{V_i}{\varphi^{m_i} S_w^{m_i}} \Rightarrow \bar{S}_w^{n_\perp} = \left(\bar{\varphi}^{m_\perp} \sum_{i=1}^k \frac{V_i}{\varphi^{m_i} S_w^{m_i}} \right)^{-1} \quad (\text{C.15})$$

finally leading to

$$n_\perp = - \frac{\ln(\bar{\varphi}^{m_\perp} \sum_{i=1}^k [V_i / (\varphi^{m_i} S_w^{m_i})])}{\ln \bar{S}_w} \quad (\text{C.16})$$

ABOUT THE AUTHORS

David Kennedy is currently a practicing formation evaluationist working for ExxonMobil International Ltd. Dave served as a research associate at ExxonMobil Upstream Research Company for three years subsequent to Exxon's and Mobil's merger. Prior to that there were 13 years at Mobil, both in research and operation services. His sojourn in the oil patch began in 1973 when Schlumberger was one of the few companies with the foresight to recruit newly-minted Georgia Tech physics graduates. After a five-year stint with Schlumberger in the field in California and Alaska, and a brief flirtation with ARCO in Dallas, a full-blown romance with graduate studies developed. David acquired MS degrees in Physics and Earth Sciences from the University of Texas at Dallas, but then jilted UTD for an infatuation with U. C. Berkeley, spending four fruitful years there but leaving without a PhD, jilted in his own turn. David has also worked briefly for Sohio and for Lockheed Missiles and Space Systems. All this activity served an interest in acquiring, understanding, and interpreting borehole resistivity measurements. At Mobil David championed the use of resistivity modeling as a routine element of log interpretation. He has studied petrophysics for years under his esteemed mentor, D. C. Herrick. Dave has five patents and 19 publications and has been internationally known as an expert in induction logging technology. He is Honorary Professor of Engineering at the Xi'an Petroleum Institute in Xi'an, China. Lately, David has had the pleasure of serving the industry from 1998 to 2002 as editor of the well logging professional journal, *Petrophysics*. He resides in Weybridge, near London, with his two darling children and his gracious and lovely mate.

David C. Herrick has recently joined Baker Atlas as Chief Petrophysicist in the Houston Technology Center. Dave was trained in chemistry and geochemistry at Indiana University (BS) and Penn State (PhD). He has conducted research, training and technical service during his twenty-five years in the petroleum industry for Conoco, Amoco and Mobil in the areas of geochemistry, petrology and petrophysics. His research interests included resistivity interpretation as a function of pore geometry and mineralogy, nuclear magnetic resonance laboratory studies and log interpretation, and capillary properties of reservoir rocks. Dave has been Training Coordinator and instructor for Amoco's well-known Petrophysics Training Program as well as an SPWLA Distinguished Speaker for three years with over forty presentations on resistivity interpretation and NMR logging given world-wide. He has been an organizing committee member for four SPWLA Topical Conferences and SPE Forums. His publications include new and fundamental work on interpretation methods for resistivity data as well as two patents.